

On the Nature of Stars with Planets

I. Neill Reid¹

*Space Telescope Science Institute, 3700 San Martin Drive, Baltimore, MD 21218;
Department of Physics and Astronomy, University of Pennsylvania, 209 South 33rd Street,
Philadelphia, PA 19104*

inr@stsci.edu

ABSTRACT

We consider the metallicities and kinematics of nearby stars known to have planetary-mass companions in the general context of the overall properties of the local Galactic Disk. We have used Strömberg photometry to determine abundances for both the extrasolar-planet host stars and for a volume-limited sample of 486 F, G and K stars selected from the Hipparcos catalogue. The latter data show that the Sun lies near the modal abundance of the disk, with over 45% of local stars having super-solar metallicities. Twenty of the latter stars (4.1%) are known to have planetary-mass companions. Using that ratio to scale data for the complete sample of planetary host stars, we find that the fraction of stars with extrasolar planets rises sharply with increasing abundance, confirming previous results. However, the frequency remains at the 3-4% level for stars within ± 0.15 dex of solar abundance, and falls to $\sim 1\%$ only for stars with abundances less than half solar. Given the present observational constraints, both in velocity precision and in the available time baseline, these numbers represent a lower limit to the frequency of extrasolar planetary systems. A comparison between the kinematics of the planetary host stars and a representative sample of disk stars suggests that the former have an average age which is $\sim 60\%$ of the latter.

Subject headings: planetary systems: formation; Galaxy: stellar content

1. Introduction

The discovery of the first extrasolar planetary system stands as one of the key scientific and philosophical advances of the twentieth century. While the existence of other planetary

systems had been postulated for several centuries (Dick, 1998), and could even be regarded as likely, particularly following the detection of circumstellar disks around young stars (see Sargent & Beckwith, 1993), Mayor & Queloz’ (1995) radial velocity measurements of 51 Pegasi marked a definitive transition from speculation to observation. The relatively short time interval which has elapsed since that initial discovery has seen the identification of a plethora of additional systems, notably by Marcy, Butler and collaborators. Taken together, those systems provide sufficient numbers for a statistical comparison of the characteristics of stars with planetary-mass companions against the overall distribution of properties of the local Galactic Disk. The results of such a study have obvious implications for estimating the likely frequency of extrasolar planets (ESPs), particularly potentially habitable systems.

Comparative studies of this type must pay due regard to several important caveats. First, it is clear that most of the ESP systems discovered to date bear little resemblance to our own Solar System: 51 Pegasi-like systems feature ‘hot jupiters’, Jovian-mass planets in sub-Mercurian orbits, while over half of the current ESP catalogue have orbital eccentricities comparable to, or exceeding, that of Mercury and Pluto. Those circumstances, however, may at least partly reflect observational selection; these systems have relatively short periods and relatively high velocity amplitudes, and are therefore the easiest to detect. All of the ‘hot jupiter’ ESPs have reflex motions of tens of ms^{-1} , and it seems likely that we have a fairly complete census of these objects. However, it is only now that observations are achieving both the requisite velocity precision and the decade-plus time baselines which are required for the detection of Jovian analogues, and systems bearing a closer resemblance to the Solar System are starting to emerge amongst the most recent discoveries (Vogt *et al.*, 2001). Thus, it is possible that the properties of the current ESP catalogue may reflect extreme, rather than characteristic, systems.

By the same token, it seems likely that the present catalogue includes only a subset of extrasolar planetary systems in the Solar Neighbourhood. Studies estimate that between 3 and 5% of F, G-type stars have currently-detectable ESP systems (Marcy & Butler, 2000). Tabachnik & Tremaine (2001), in particular, have used maximum-likelihood analysis to estimate that current observations indicate a planetary frequency of 3% amongst solar-type stars, but that the frequency might be as high as 15% if the companion mass function is extrapolated to terrestrial-mass systems. Thus, the observed detection frequency may well underestimate the true frequency of solar-type stars with planetary systems, and possibly provides a biased sampling of their characteristics.

Nonetheless, the current dataset offers a first cut at determining the conditions required for the formation of planetary systems. How are the ESP primaries distinguished from the average local field star? Studies to date have focused on chemical abundance, with strong

indications that stars known to have planets tend to have solar or super-solar metallicity (Gonzalez, 1998; Santos et al, 2001). While this may indicate a requirement on the initial conditions at formation, there have also been suggestions that these higher abundances are a consequence of planet formation (Lin *et al.*, 1996), reflecting pollution of the stellar atmosphere by migrating gas giants (Gonzalez, 1997; Laughlin, 2000).

Placing this result in the broadest context requires consideration of both correlations which might exist with other properties of the planetary host stars, and comparison against data for a reliable reference sample of representative disk stars. The latter criterion is not met in some recent analyses. In this paper we re-examine the abundance distribution of the ESP hosts, matched against similar data for an Hipparcos-based, volume-limited sample of FGK stars. We also compare the kinematics of ESP hosts against the velocity distribution of local disk stars. The paper is organised as follows: the following section presents basic data for the ESP host stars; section 3 discusses abundance calibration and the metallicity distribution; section 4 examines the kinematics of the sample; and section 5 summarises our main conclusions.

2. The planetary hosts in the HR diagram

2.1. The sample

Table 1 lists basic photometric and parallax data for stars currently known to possess at least one planetary-mass companion. We shall refer to those stars as ESP host stars. In compiling this list, we follow the Geneva convention (<http://obswww.unige.ch/udry/planet/>) of setting an upper mass limit of $M_2 \sin i = 17M_J$, where M_J is the mass of Jupiter. There are only four systems where $M_2 \sin i$ exceeds $10M_J$. The parameters listed for the planetary systems are taken from the Extrasolar Planets Encyclopedia maintained by J. Schneider at <http://cfa-www.harvard.edu/planets/>.

Since we only measure $M_2 \sin i$ for most of these systems, there is clearly potential for the inclusion of higher-mass companions on low-inclination orbits, either low-mass stars or brown dwarfs. Indeed, there may well be an overlap between the upper mass range of planets and the lower mass-range of brown dwarfs¹, leading to an inherent ambiguity in interpretation. Since those two classes of objects may have different intrinsic properties, it is important to

¹In making this statement, we define planets as forming in a circumstellar disk, while brown dwarfs form as independent accreting cores in the parent molecular cloud. Following common usage, we also require planets to be in orbit around a more massive central body. Other definitions of these terms are possible.

consider the likely level of cross-contamination.

The degree of contamination depends on the prevalence of brown dwarfs as close companions to solar-type stars. Few unequivocal examples of such systems have been detected, leading both to the postulation of a ‘brown dwarf desert’ at $a < 10$ a.u. (Marcy & Butler, 2000), and support for the hypothesis that the low mass ($M_2 \sin i < 10M_J$) companions that are detected are not a simple extension of the companion mass function at higher masses. On the other hand, there have been counter suggestions. Both Heacox (1999) and Stepinski & Black (2000) have pointed out the similarity between the orbital properties of planetary-mass systems and stellar binaries, although that might reflect similar dynamical evolution rather than similar origins. More directly, Han *et al.* (2000) and Gatewood *et al.* (2000) have analysed radial velocity data in tandem with Hipparcos Intermediate Astrometric Data, and claim that in many cases the best-fit orbits have low inclination, and correspondingly high true masses in the brown dwarf or even stellar régime.

The Han *et al.* result has been scrutinised intently and generally found wanting. Statistically, the scarcity of systems with $M_2 \sin i > 15 M_J$ demands a rather unlikely observational conspiracy, with orbital axes aligned within a few degrees of the line of sight. Under a random distribution of inclinations, one would expect several hundred systems with brown-dwarf mass companions for each planetary-mass system; not only are the latter systems not observed, but there are not sufficient G dwarfs in the Solar Neighbourhood to meet the numerical requirements. The amplitudes of the derived astrometric orbits are comparable with the uncertainties in the Hipparcos IAD measurements, and Pourbaix (2001) has shown that the low inclinations found by Han *et al.* are largely an artefact of the fitting technique used. Pourbaix & Arenou (2001) conclude that ρ CrB is the only system where the data merit interpretation as a near face-on orbit, but HST astrometry by McGrath *et al.* (2001) sets an upper limit on the semi-major axis at $a \sin i < 0.3$ milliarcseconds (mas) corresponding to $M_2 < 30M_J$, rather than the 1.5 mas and $0.14 \pm 0.05M_\odot$ suggested by Gatewood *et al.* (2000).

Current estimates of the companion mass function are generally in good agreement, finding approximately equal numbers per decade in mass ($\frac{dN}{dM} \propto M^{-1}$) for $M < 10M_J$, with a sharp drop at higher masses (Jorissen *et al.*, 2001; Zucker & Mazeh, 2001; Tabachnik & Tremaine, 2001). Indeed, astrometric observations have shown that many of the candidate brown dwarf companions are, in fact, low-mass M dwarfs (Halbwachs *et al.*, 2000), further enhancing the brown dwarf desert. Based on these results, we expect little contamination (<5%) in the ESP sample listed in Table 1. Nonetheless, one star deserves comment. As discussed later, HD 114762 is one of the most metal-poor stars in the sample. The measured stellar rotational velocity suggests that the star is being viewed close to pole-on, implying a

low inclination for an equatorial orbit. In that case, the companion, detected by Latham *et al.* (1989) is a candidate for the first brown dwarf identification.

2.2. The (M_V , (B-V)) colour-magnitude diagram

All of the stars except BD -10 3666 were observed by Hipparcos, and most have trigonometric parallaxes measured to an accuracy of better than 5%. The BV photometry listed in Table 1 is also taken from the Hipparcos catalogue (ESA, 1997), although we use the literature data cited therein in preference to Tycho photometry, given the systematic offset (and occasional large random errors) between the latter system and standard Johnson data (Bessell, 2000). BD -10 3666 has UVB photometry by Ryan (1992) but no measured trigonometric parallax, and the absolute magnitude listed in Table 1 is based on an estimated photometric parallax. Since both this star and HD 4203 were selected for observation based on the known high metallicity, neither plays a role in the statistical comparison discussed in the following sections.

The photometry and astrometry listed in Table 1 allow a detailed assessment of the distribution of the ESP host stars in the HR diagram. Figure 1 makes that comparison, where the reference main sequence is provided by data for stars within 25 parsecs which have accurate photometry and trigonometric parallaxes measured to a precision of $\frac{\sigma_\pi}{\pi} < 10\%$. All of the latter stars are members of the Galactic Disk. Three features are immediately noticeable:

1. G dwarfs contribute the majority of planet detections, with Gl 876 still the only M dwarf known to have planetary-mass companions. To a large extent, the distribution likely reflects the continuing observational focus on solar-type stars.
2. The current sample includes a significant number of evolved stars. At least six stars lie at the base of the subgiant branch, while four have evolved a considerable distance from the main sequence. These stars are identified in Table 1.
3. The ESP host stars are distributed throughout the full width of the main sequence. This is important since chemical abundance is the dominant factor which governs the location of single stars on the main sequence - at a given colour, metal-rich stars are more luminous than metal-poor stars. Thus, the observed distribution points to a range of metallicity amongst stars with planets which is at least comparable to the abundance distribution amongst the underlying local disk (thin+thick) population.

The last point is particularly pertinent given the recent emphasis laid on the high metal

abundance measured for at least some of the ESP primaries (Gonzalez *et al.*, 1999, 2001; Santos *et al.*, 2001). Many of those abundances are significantly higher than the value usually taken as the median for the Galactic Disk. Most previous studies, however, treat the metallicity distributions of the ESP hosts and of the disk as separate entities. The following section places the former in the context of the latter, and considers how the high chemical abundances are reconciled with the distribution evident in Figure 1.

3. Chemical abundances

3.1. Measuring stellar metallicity

The metal content of stellar atmospheres can be measured using a wide variety of techniques. In general, the accuracy of the final measurement is at least inversely proportional to the difficulty of the observation. Analyses based on high-resolution spectroscopy are usually more reliable than those which utilise broadband colours, but photometric data are obtained much more readily than echelle spectra. Thus, any statistical analysis requiring a dataset of even modest dimensions must balance two factors - availability and accuracy.

As a further complication, comparative studies must ensure that data drawn from different analyses are tied to a consistent system. Different measurement techniques not only have different random uncertainties, but can also exhibit systematic discrepancies in scale and/or zeropoint, as discussed in the context of globular cluster distance determination by Gratton *et al.* 1997) and Reid (1998). Apart from differences in the choice of standard stars, we note that the solar iron abundance was re-calibrated relatively recently, revised downward from $A(\text{Fe})=7.67$ to $A(\text{Fe})=7.54$ (Biemont *et al.*, 1991), where $A(\text{Fe})$ is the logarithmic abundance on a scale where $A(\text{H})=12$. While most abundances are measured differentially, this re-calibration might lead to a systematic offset depending on how and when the abundances of the standard stars were determined.

This issue is a concern since, while nearly all of the ESP host stars have recent high-resolution spectroscopic abundance measurements, most estimates of the underlying field-star metallicity distribution rest on lower resolution techniques. Santos *et al.* (2001) have addressed this problem to some extent by providing high-resolution spectral analyses for 43 G dwarfs in 42 systems drawn from the volume-limited sample of stars with $(B-V) < 1.1$ and $d < 17$ parsecs. That sample is scarcely sufficient in size, however, to provide an adequate mapping of the distribution of disk properties. We adopt an alternative strategy in this paper.

Strömgren uvby photometry provides a relatively simple means of determining abun-

dances for F, G and early K-type stars (Strömgen, 1966). Data are available for most solar-type stars brighter than 10th magnitude. Indeed, both Giménez (2000) and Laughlin (2000) have applied those measurements to studying the ESP host stars. Metallicities are determined by measuring the differential line-blanketing via the m_1 and c_1 indices, where

$$m_1 = (v - b) - (b - y)$$

and

$$c_1 = (u - v) - (v - b)$$

The latter index is also gravity sensitive, allowing discrimination between dwarfs and subgiants.

The literature contains several calibrations of the Strömgen indices against metallicity. Giménez adopts that given by Olsen (1984); we follow Laughlin in using the more recent calibrations derived by Schuster & Nissen (1989). They provide two calibrating relations,

$$\begin{aligned} [Fe/H]_{uvby} = & 1.052 - 73.21m_1 + 280.9m_1(b - y) + 333.95m_1^2(b - y) - 595.5m_1(b - y)^2 \\ & + [5.486 - 41.61m_1 - 7.963(b - y)] \times \log (m_1 - [0.6322 - 3.58(b - y) + 5.20(b - y)^2]) \end{aligned}$$

for F stars, ($0.22 \leq (b - y) < 0.375$, $0.03 \leq m_1 \leq 0.21$, $0.17 \leq c_1 \leq 0.58$ and $-3.5 \leq [Fe/H] \leq 0.2$), and

$$\begin{aligned} [Fe/H]_{uvby} = & -2.0695 - 22.45m_1 - 53.8m_1^2 - 62.04m_1(b - y) + 145.5m_1^2(b - y) \\ & (85.1m_1 - 13.8c_1 - 137.2m_1^2)c_1 \end{aligned}$$

for G stars ($0.375 \leq (b - y) \leq 0.59$, $0.03 \leq m_1 \leq 0.57$, $0.10 \leq c_1 \leq 0.47$ and $-2.6 \leq [Fe/H] \leq 0.4$).

Apart from BD -10 1366 and Gl 876, where Strömgen data offer little useful information, only HD 177830 (HIP 93746) lacks uvby photometry. Table 2 lists (b-y), m_1 and c_1 colour indices, taken from Hauck & Mermilliod’s (1998) catalogue, and the resulting $[Fe/H]_{uvby}$ for the remaining stars, together with the metallicities derived from high-resolution spectroscopy. As expected, there is a systematic offset to lower abundances in the Strömgen calibration. The results are compared in Figure 2, where the upper panels plot the full dataset (see also Figure 1 in Laughlin, 2000). We note that residuals tend to increase among early-type K stars, $(b-y) > 0.5$, where both methods become more problematic.

We have quantified the comparison using the datasets from Santos *et al.* (2001) and Gonzalez and collaborators, which provide two internally consistent datasets of moderate size. Based on the twenty-two ESP host stars observed by Santos *et al.* (2001), we derive

$$\delta[Fe/H] = [Fe/H]_{uvby} - [Fe/H]_{sp} = -0.117 \pm 0.095$$

where the uncertainties quoted are the rms dispersion about the mean. The formal standard error of the mean, σ_μ , is 0.020 dex and the median offset is -0.13 dex. The twenty-two stars in the Gonzalez dataset give an almost identical result,

$$\delta[Fe/H] = -0.118 \pm 0.113, \quad \sigma_\mu = 0.024$$

The median offset is -0.10 dex. Combining both datasets with forty field stars from the Santos *et al.* reference sample gives

$$\delta[Fe/H] = -0.083 \pm 0.118, \quad \sigma_\mu = 0.013$$

The median offset is -0.07 dex. This is in excellent agreement with Gratton *et al.*'s independent analysis of 152 stars spanning a much larger range of metallicity, where they derive

$$\delta[Fe/H] = -0.102 \pm 0.151, \quad \sigma_\mu = 0.012$$

Given uncertainties of ± 0.06 dex in the Santos *et al.* and Gonzalez spectroscopic measurements, the measured dispersion indicates that the Strömngren data have typical uncertainties of ± 0.1 dex at near-solar abundances, sufficient accuracy for present purposes.

Based on this comparison, we conclude that the Strömngren abundance scale is offset by -0.1 dex from the most recent calibrations. We note that the offset is intriguingly similar to the re-calibration of the solar abundance, although that similarity may be coincidental. Rather than attempt to correct the metallicity measurements, we base our analysis on the *uvby* scale; in effect, we adopt the somewhat paradoxical definition

$$[Fe/H]_{uvby}(\odot) = -0.1$$

Since we are considering the comparative distributions of field star and ESP host star abundances, consistency is more important than the numerical value chosen for the fiducial zero-point.

3.2. The reference sample

Defining a suitable reference sample is crucial to assessing how the properties of the ESP host stars map onto the overall field star distribution. Complete, volume-limited datasets offer the most reliable comparison, but have generally not been available to previous studies. Murray *et al.* (2001) have attempted to turn Hipparcos data to this end, with a reference sample defined by selecting HD stars with $\pi > 10$ mas and $\frac{\sigma_\pi}{\pi} < 10\%$. However, the colour-magnitude diagram for this dataset (Figure 1 in Murray & Chaboyer, 2001) is clearly biased

strongly towards F-type and early G-type dwarfs, partly reflecting sampling in the Hipparcos catalogue at $V > 9$ th magnitude, and partly reflecting the fact that the HD catalogue was selected from blue photographic plates. The resulting dataset therefore provides a biased subset of nearby disk stars. Murray *et al.*'s metallicities are taken from the Cayrel de Strobel (1997) catalogue, and therefore represent an amalgam of heterogenous sources. Thus, this dataset is not suitable as a local reference.

Several other analyses (e.g. Gonzalez, 1999; Butler *et al.*, 2000) have relied on the nearby-star sample defined by Favata *et al.* (1997: F97) to represent the abundance distribution of local disk stars. That sample, however, is severely flawed in several important respects, as illustrated in Figure 3. The F97 abundances are derived from high-resolution spectra, and a comparison with Strömgren abundances gives

$$\delta[Fe/H] = -0.05 \pm 0.15, \text{ 69 stars}$$

somewhat less than the offsets derived in the previous section. The full sample of 90 stars includes both components of several binaries, giving those systems double weight in the abundance distribution, and spans a substantially larger colour range than ESP host stars (excluding Gl 876). Finally, and most significantly, the sample is neither complete nor volume-limited. Favata *et al.* (1996) constructed the original sample by taking a randomly-selected subset of 200 stars with $0.5 < (B - V) < 1.4$ from the second Catalogue of Nearby Stars (Gliese, 1969; Gliese & Jahreiß, 1979: CNS2). Ninety-four of those stars were observed spectroscopically. Unfortunately, while the CNS2 has a nominal distance limit of 25 parsecs, subsequent Hipparcos astrometry has shown that a significant fraction of the stars lie at much larger distances. Figure 3 shows that at least 40% of the F97 dataset lies beyond 25 parsecs. Our analysis demands a more reliable reference dataset.

Figure 4 shows the $(M_V, (B-V))$ colour-magnitude outlined by the 1549 stars in the Hipparcos catalogue with formal trigonometric parallax measurements exceeding 40 mas ($d \leq 25$ parsecs, $(m-M) \leq 1.99$). As in Figure 1, we use the literature BV photometry in the catalogue in preference to Tycho data. We have not applied any cut based on parallax precision, but use different symbols to identify the 1477 stars with parallaxes measured to a precision of better than 20%. Nearly all of the stars lying below the main-sequence in this figure have inaccurate parallax measurements.

The box superimposed on Figure 4 isolates 488 stars with $0.5 \leq (B - V) \leq 1.0$ and $2.0 \geq M_V \geq 7.0$, matching the colour/magnitude range of the bulk of the ESP host stars. The limiting magnitude for completeness in the Hipparcos catalogue is

$$V = 7.9 + 1.1\sin|b|$$

so the 25-parsec sample is effectively complete over the whole sky for $M_V \leq 5.9$ (the dotted line in Figure 4). The full catalogue is $\sim 25\%$ incomplete for stars with $8 \leq V < 9$, but should be significantly more complete for nearby stars, since all stars suspected of being within 25 parsecs were included in the input catalogue - as emphasised by the large numbers of M dwarfs in Figure 4. Indeed, Jahrei & Wielen (1997) argue that the Hipparcos catalogue is essentially complete to $M_V = 8.5$ for stars within 25 parsecs of the Sun. Thus, the F, G and K stars isolated in Figure 4 effectively represent a complete, volume-limited sample. We identify these stars as the FGK25 Hipparcos dataset. Note that the sample includes 20 known ESP hosts from Table 1.

As noted in the previous section, Strmrgren photometry is now available for a substantial number of bright F, G and K stars, and is readily accessible through the catalogue compiled by Hauck & Mermilliod (1998). We have cross-referenced the FGK25 Hipparcos dataset against that catalogue and located photometry for 419 of the 486 stars - 86% of the sample. Those stars are identified as solid squares in Figure 4. The sample includes members of binary systems, but only one star per system. It is clear that almost every star with $(B-V) < 0.8$ has photometry, while the late-G and K dwarfs which lack Strmrgren measurements are distributed over the full width of the main sequence, interspersed with stars which have uvby photometry. We conclude that the abundance distribution deduced from these data is characteristic of the parent population(s) of the ESP host stars.

3.3. The abundance distribution of local field stars

The overwhelming majority of the stars in the FGK25 sample are members of the Galactic Disk. Five stars, however, lie significantly below the main sequence. These are HIP 57939, 62951, 67655, 79537 and 79979. Two of these stars, HIP 62951 and HIP 79979, are in binary systems where the companion has affected the parallax determination; Fabricius & Makarov (2000) have reanalysed the Hipparcos data for HIP 62951 and find $\pi = 2.4$ mas. These are the only two stars in the FGK25 sample with $\frac{\sigma_\pi}{\pi} > 0.2$ (there are only 6 other stars with $\frac{\sigma_\pi}{\pi} > 0.1$), and we exclude both from our sample. The remaining three subluminoous stars are *bona-fide* metal-poor subdwarfs. HIP 57939 is HD 103095, or Groombridge 1830, the well-known intermediate-abundance ($[\text{Fe}/\text{H}]_{uvby} = -1.4$) subdwarf; HIP 67655, or HD 120559, has $[\text{Fe}/\text{H}]_{uvby} = -0.94$; and HIP 79537 is HD 145417, $[\text{Fe}/\text{H}]_{uvby} = -1.25$. The presence of three such stars in this volume-limited sample suggests a somewhat higher density normalisation ($(\sim 0.6 \pm 0.35)\%$ relative to the disk population) than usually adopted for the local Galactic

halo².

Before comparing these results against other recent analyses, we should emphasise the limited nature of the present study. The question addressed here can be stated as follows: Based on current statistics, and given a sample of stars drawn from the Galactic mid-Plane near the Sun, what is the frequency of ESP systems as a function of metallicity.

Our goal in constructing the reference sample of field stars, therefore, is not an unbiased estimate of the present-day metallicity distribution of the Galactic Disk - a parameter used to constrain Disk star formation histories. That undertaking requires limiting analysis to stars with main-sequence lifetimes older than the age of the Disk, avoiding possible bias through a disproportionate contribution from recent star formation episodes. Moreover, given a potential correlation between metallicity and velocity, one should weight each star's contribution by its W-velocity to allow for the residence time in the mid-Plane and convert volume density to surface density. The latter is not an option for the present sample, since over 25% of the stars lack radial velocities. Moreover, our (B-V) limits, modelled on the known ESP systems, include early-type G and late-F stars, whose main-sequence lifetimes are shorter than 10 Gyrs. Thus, our field star sample is tailored to provide a local snapshot of the present-day abundance distribution in the mid-Plane, rather than an integrated history of star formation in the Disk.

We have compared the abundance distribution of the FGK25 dataset against results from two other studies: the Favata *et al.* (1997) analysis, described above, and the recent study by Haywood (2001: H2001). In both cases, we consider volume-limited samples (i.e. the distribution is not weighted by W velocity as in Figure 3 of F97). Haywood's analysis is aimed at determining an unbiased estimate of the Disk abundance distribution, so while his initial sample is selected to have $M_V < 8.5$, $(B-V) > 0.25$ and $\pi > 40$ mas (based on Hipparcos data), the final analysis is limited to 328 stars with $M_V > 4.5$; that is, main-sequence dwarfs with lifetimes longer than the age of the Disk. Abundances are derived primarily from Geneva photometry, supplemented by Strömgren data, with the metallicity scale effectively adjusted to the high-resolution (Santos/Gonzalez) system.

Figure 5 compares the abundance distributions derived in those studies against our own results. For consistency, we have adjusted all of the metallicity scales to match $[Fe/H]_{uvby}$. All three distributions peak at values close to the solar abundance, with a substantial fraction of the sample (45% in the FGK25 dataset) having super-solar metallicities. As discussed

²This has implications for the interpretation of the nature of the cool white dwarfs identified in recent proper motion surveys (Oppenheimer *et al.*, 2001). An increased local density of the *stellar* halo easily accounts for the observed numbers of high velocity stars, as suggested by Reid *et al.*, 2001).

by Haywood, this represents a significant revision of previous analyses, and may reflect a bias against metal-rich stars in samples selected based on spectral type rather than distance/colour. We note that only a small fraction of the local Disk have abundances of less than $\frac{1}{3}$ solar: only 25 stars (6%) in the FGK25 sample. If $\approx 10\%$ of the local stars are members of the thick disk, as suggested by kinematic analyses (Reid, Hawley & Gizis, 1995), then the mean abundance of that sub-population lies much closer to the solar metallicity than the value of $[\text{Fe}/\text{H}]=-0.6$ adopted in some Galactic models.

Both the F97 and H2001 samples show a more extended distribution towards higher abundances than the FGK25 dataset. This is somewhat surprising, since the latter sample, extending to stars brighter than $M_V = 4$, should include a higher proportion of younger stars which are likely to be more metal-rich. The discrepancy may originate from the abundance calibrations. Figure 6 shows the metallicity distribution as a function of (B-V) colour for the H2001 and FGK25 datasets. The former shows a clear trend of increasing metallicity at redder colours, suggesting a possible systematic bias in the abundance calibration of Geneva photometry. Further observations are required to verify this hypothesis.

For present purposes, the most significant point is that the metallicities discussed here for both field stars and ESP host stars are derived from a single source - Strömgren photometry, as calibrated by Schuster & Nissen (1989). Thus, the comparison between the two abundance distributions described in the following section is internally fully self-consistent.

3.4. The abundance distribution and the frequency of giant planets

Before comparing metallicities, Figure 7 matches the $(m_1, (b-y))$ and $(c_1, (b-y))$ distributions of the ESP host stars and the FGK25 Hipparcos sample. We have distinguished between main sequence stars and potential subgiants in the former sample. As previously noted by Giménez (2000), a significant fraction of the ESP host stars have high c_1 values, suggesting low gravities and a mildly evolved status. In some cases, however, the colours reflect high metallicity rather than low gravity; thus, both HIP 43587 (55 Cnc) and 79248 (HD 145675) lie well above the $((b-y), c_1)$ sequence at $(b-y)\sim 0.42$, but their location in the $(M_V, (B-V))$ plane demands that both are main-sequence dwarfs. Spectroscopy indicates that both are super-metal rich (Table 2). Nonetheless, the fraction of subgiants amongst known ESP hosts ($\sim 15\%$) is at least a factor of three higher than that in the volume-limited sample. This may reflect an observational selection effect, since evolved stars are intrinsically more luminous, and therefore more likely to be included in the radial velocity monitoring programs.

The reddest star in the sample is the K2 subgiant, HD 27442 (HIP 19921). This lies beyond the formal limits of the Schuster & Nissen (1989) abundance calibration, at (b-y)=0.65; however, the derived metallicity, $[\text{Fe}/\text{H}]_{uvby}=0.26$, is not inconsistent with the spectroscopic determination of $[\text{Fe}/\text{H}]=+0.22$, so we have retained the star in the sample. We have excluded both BD -10 1366 and HD 4203 from the statistical comparison. As noted above, those stars were added to the Keck/Lick radial velocity program because they were known to be extremely metal-rich. The M dwarfs, Gl 876, is also excluded, but we include HD 177830, adjusting its abundance from $[\text{Fe}/\text{H}]=0.36$ to $[\text{Fe}/\text{H}]_{uvby}=0.26$.

The sample of ESP host stars is not volume-limited, particularly given the fact that the original target list was constructed before the availability of Hipparcos data, and is therefore subject to the type of distance errors illustrated in Figure 3. There may therefore be underlying biases reflecting the initial selection of which stars to monitor. Those effects can be quantified once the full dataset is available. Nonetheless, it is not unreasonable to hope that the current catalogue of ESP host stars provides a representative subset of stars with currently-detectable planetary systems; that is, stars with relatively massive (super-Jovian) companions on relatively short-period (< few years) orbits.

Figure 8 plots the abundance distribution of both the ESP host stars and the reference FGK25 Hipparcos dataset. The subgiant contribution to the former distribution is shown as the shaded histogram and is consistent with the overall distribution. As emphasised in §3.1, these data are all on the Strömgren system, $[\text{Fe}/\text{H}]_{uvby}$, placing the Sun as -0.1 dex, at the mode of the local abundance distribution.

Visual comparison clearly confirms previous suggestions that the abundance distribution of the ESP host stars is weighted more heavily towards super-solar metallicity than the field distribution. To quantify that comparison we have combined the distributions by scaling the upper distribution to match the observed fraction of ESP hosts amongst the volume-complete sample. As noted above, 20 of the 486 stars in the FGK25 sample, or 4.1%, are known to have planetary-mass companions. This fraction is broadly consistent with previous estimates (e.g. Marcy & Butler, 2000). We have used this factor to scale the metallicity distribution in the uppermost panel of Figure 8, and the two lowest panels in Figure 8 show the fraction of ESP host stars,

$$f_{ESP} = \frac{N_{ESP}}{N_{tot}}$$

as a function of metallicity. There is an obvious trend with abundance, with f_{ESP} rising to near unity at the highest abundances; both of the stars in the highest-metallicity bin of the FGK25 sample are known to have planetary-mass companions. However, even at an abundance of $\frac{2}{5}$ th solar, $\sim 1\%$ of F, G and early-K stars are predicted to have Jovian-mass planetary companions. HD 114762b, the likely brown dwarf, contributes the spike at

$[\text{Fe}/\text{H}]_{uvby} = -0.7$ dex.

Finally, we have compared the properties of the individual planetary systems against the abundances derived from the Strömgren data. Figure 9 shows the results, where we identify separately systems with multiple components (including the Sun, represented by Jupiter and Saturn). There is no obvious correlation between $[\text{Fe}/\text{H}]_{uvby}$ and any of the observed characteristics.

3.5. Discussion

Is the correlation with metallicity evident in Figure 8 a selection effect? Metal-rich stars are more luminous than their metal-poor counterparts, and therefore, like subgiants, might be expected to be better represented in a target list which is partly magnitude limited. However, it seems unlikely that this type of bias could account for the smooth trend evident in the observations, particularly given the identification of planetary companions to BD -10 1366 and HD 4203, stars specifically added to the Keck program because they were known to be super-metal-rich. Thus, the simplest interpretation of Figure 8 is that the correlation represents a real physical phenomenon. The explanation for this phenomenon is somewhat less clear.

Perhaps appropriately, the two mechanisms proposed to account for the observed correlation mirror the classic nature *versus* nurture debates of biological behavioural sciences. Under the first hypothesis, planetary systems (at least those with giant planets) form more readily in the dustier environment likely to be present in high-metallicity circumstellar disks. Under the alternative hypothesis, gas giants migrate inwards due to dynamical friction with residual disk material and are absorbed into the stellar envelope. The enhanced metal content of the planet (solar system giants are likely to have $Z > 0.1$) enriches the metallicity of the outer convective envelope, leading to a higher measured chemical abundance.

One question mark hanging over the planetary pollution hypothesis centres on the details of the enhanced metal content of Jovian planets. In astronomical terms, ‘metals’ encompass all elements except hydrogen and helium - but not all metals are created equal. Metallicity measurements for F, G and early K-type stars are primarily measuring blanketing due to heavy elements, notably iron. The giant planets are known to have non-cosmic inter-element abundance ratios, but if the additional ‘metals’ are ices (C, N, O) rather than minerals (Fe, Si, Ni), as suggested by the possible absence of a rocky core in Jupiter (Guillot, 1999), then planetary pollution will have little effect on the apparent metallicity of the stellar envelope.

These two competing scenarios are discussed extensively by, amongst others, Gonzalez

(1997, 1999), Laughlin (2000), Murray *et al.* (2001) and Santos *et al.* (2001). A major prediction of the pollution hypothesis is that the degree of metallicity enhancement should increase with increasing mass of the parent star. This follows from the corresponding decrease in mass of the convective envelope; adding high-Z material gives a proportionately larger increase in metallicity. Both Laughlin and Murray & Chaboyer (2001) have argued that this effect is present, although the latter authors note that a similar trend is present in their reference sample, and both analyses are based on a subset of the current catalogue of ESP hosts. Santos *et al.* (2001), in contrast, arrive at the opposite conclusion based on analysis of more than 60 systems. In their analysis, they rightly place more emphasis on the location of the upper envelope of the abundance distribution as a function of mass, rather than the mean metallicity.

All three of these analyses use theoretical tracks to deduce masses for individual ESP host stars. Figure 10 shows an alternative, more empirical approach. We have separated the current sample into main-sequence stars and subgiants based on location in Figure 1, and plot the abundance as a function of (b-y). For the main-sequence sample, (b-y) effectively traces mass, and the absence of any strong trend in the location of the high-metallicity boundary, in particular, a decrease in $[\text{Fe}/\text{H}]_{max}$ at redder (b-y) colours, supports the conclusion reached by Santos *et al.* Moreover, the latter authors point out that as stars evolve onto the subgiant branch, the convective envelope increases in size, diluting the effect of any planetary pollution. It is clear from Figure 10 that the evolved stars can be as metal-rich as the main-sequence dwarfs; indeed, the K2 subgiant HD 24427 (HIP 19921) is amongst the most metal-rich stars in the sample. Thus, these results suggest that planetary systems are born metal-rich, rather than having high metallicity thrust upon them.

4. Kinematics

4.1. Velocity dispersion and ages

The age distribution of the ESP host stars is clearly an important parameter for understanding the Galactic origins of these systems. Two techniques have been used to estimate ages for individual stars: isochrone fitting; and the level of chromospheric activity, as measured through emission at the Ca II H & K lines. Both methods can be applied to individuals, but both have limitations. Isochrone fitting provides reliable ages for relatively F and early-G stars, but becomes less accurate for longer-lived, later-type stars. Chromospheric ages, quantified using the R'_{HK} index (Soderblom *et al.*, 1991), are more readily derived, but are also less reliable since there is a considerable dispersion in activity amongst individual stars with similar ages (see Figure 10 in Soderblom *et al.*). Moreover, variability is an issue; as

Henry *et al.* (1996) point out, the Sun’s age could be estimated as anywhere between 2.2 and 8 Gyrs depending on when the observations are taken during the Solar cycle. Finally, both of these techniques become significantly less reliable at ages exceeding ~ 2 Gyrs (as evidenced by continuing uncertainties in the Galactic star formation history).

Nonetheless, both of these methods provide useful insight into the age distribution, and both have been applied by Gonzalez and co-workers (Gonzalez & Laws, 1998; Gonzalez, 1999; Gonzalez *et al.*, 2001) to estimate ages for 33 of the systems listed in Table 1. A comparison between the different estimates emphasises the inherent uncertainties, most dramatically for HD 217107 and HD 222582, where both have chromospheric age estimates of 5.6 Gyrs, but isochrone estimates of 1.2 and 11 Gyrs, respectively. Averaging the results for all 33 stars, we derive a mean age of 5.6 Gyrs ($\sigma = 3.6$ Gyrs).

Space motions cannot be used to provide age estimates for individual stars. However, stellar kinematics offer an alternative means of comparing the *average* properties of diverse groups of stars. Velocity dispersion increases with age, probably through the mechanisms of orbital diffusion (Wielen, 1977) and scattering due to molecular clouds (Spitzer & Schwarzschild, 1953). A comparison between the velocity distributions of the ESP host stars and the local disk can test whether there is a significant difference in the mean age of the two samples.

We have calculated space motions for the ESP hosts using astrometric data from the Hipparcos catalogue and the available radial velocity measurements. Table 3 lists those data and the resulting (U, V, W) motions, where U is positive toward the Galactic Centre, V positive in the direction of rotation, and W directed toward the NGP.

All of the FGK25 stars have accurate proper motions and parallaxes from Hipparcos, but only 60% have published radial velocities, rendering the sample unsuitable as a reference. However, the volume-complete M-dwarf sample from the PMSU survey of nearby stars (Reid *et al.*, 1995: PMSU1) gives a ready alternative, providing an unbiased representation of the kinematics of local disk stars. Reid *et al.* (2002: PMSU4) have revised the original dataset to incorporate more recent astrometric data, notably from Hipparcos, besides including higher-accuracy radial velocities from echelle observations summarised by Gizis *et al.* (2001: PMSU3). The final sample is comparable in size to the FGK25 dataset, with 436 systems lying within M_v -dependent distance limits ranging from 10 to 20 parsecs.

Figure 11 compares the velocity distributions of the two datasets. The left-hand panels plot the two-component velocity distributions; the right-hand panels show probability plots of the (U, V, W) distributions. As originally discussed by Lutz & Upgren (1980), these diagrams plot the cumulative distribution of a sample, $C(x)$, against the difference with

respect to the mean value, \bar{x} , in units of the standard deviation. A normal distribution, $f(x) = \frac{1}{\sqrt{2\pi}\sigma} \cdot e^{-\frac{(x-\bar{x})^2}{\sigma^2}}$, gives a straight line, slope σ , in this plane. Figure 11 plots three empirical velocity distributions: data for the ESP host stars; for the full PMSU M-dwarf sample; and for the PMSU dMe dwarfs, with H α emission exceeding 1Å equivalent width. As discussed by Hawley *et al.* (1996; PMSU2), chromospheric emission is an age-dependent phenomenon, so the last dataset is characteristic of a moderately young stellar population, $\langle\tau\rangle \approx 1 - 2$ Gyrs.

It is clear from Figure 11 that the velocity distribution of the ESP host stars is more closely matched to the full M dwarf sample than to the dMe sample. Quantitatively, linear fits to the central regions of the probability plots ($-1.9 < rms < 1.9$) give

$$(\sigma_U = 35.2; \sigma_V = 22.9; \sigma_W = 17.3 : U_\odot = -6.3; V_\odot = -24.2; W_\odot = -7.7) \\ \sigma_{tot} = 45.4 \text{ kms}^{-1}; 63 \text{ systems}$$

where σ_{tot} is the overall velocity dispersion. Applying the same technique to the M dwarf samples gives

$$(\sigma_U = 21.2; \sigma_V = 14.1; \sigma_W = 13.0 : U_\odot = -14.5; V_\odot = -11.5; W_\odot = -8.1) \\ \sigma_{tot} = 28.6 \text{ kms}^{-1}; 69 \text{ systems}$$

for the emission line dwarfs and

$$(\sigma_U = 39.1; \sigma_V = 38.8; \sigma_W = 23.6 : U_\odot = -5.7; V_\odot = -9.6; W_\odot = -3.3) \\ \sigma_{tot} = 59.9 \text{ kms}^{-1}; 404 \text{ systems}$$

for the full sample.

Based on this comparison, we conclude that the current sample of F, G and K-type ESP hosts is younger, on average, than the overall disk population, but includes stars significantly older than typical of the dMe sample. Quantitatively, if we assume diffusion with $\sigma \propto \tau^{\frac{1}{2}}$, then

$$\langle\tau_{ESP}\rangle \sim 0.6\langle\tau_{dM}\rangle \sim 2.5\langle\tau_{dMe}\rangle$$

suggesting an average age of 3-4 Gyrs for ESP host stars for an approximately uniform star-formation rate in a 10-Gyrs-old disk. This younger mean age is not unexpected, given the higher proportion of metal-rich stars amongst the ESP sample. The average metal abundance of the Galactic disk is expected to increase with time, as successive generations of star formation contribute additional nucleosynthetic debris to the interstellar medium, so a sample biased toward high metallicities is also likely to be biased towards stars that are younger than average.

4.2. Kinematics and metallicity

The previous section considered the overall distribution of velocities of the ESP host stars. We can also look for correlations using velocities for the individual stars, correcting the observed heliocentric data for the solar motion with respect to the Local Standard of Rest (LSR). For the latter parameter, we use the values derived by Dehnen & Binney (1998),

$$(U_{\odot}, V_{\odot}, W_{\odot}; 10.0, 5.3, 7.2)$$

where these values give the motion of the Sun with respect to the LSR. Thus, the Sun is moving towards the Galactic Centre, towards the direction of rotation and towards the NGP, and the observed velocities must be corrected accordingly. We denote the corrected velocities as (U', V', W') .

Figure 12 plots velocities for the ESP host stars as a function of abundance. We also indicate the location of the Sun on these diagrams. There is no obvious correlation between metallicity and either the (U', V', W') component velocities or the total motion with respect to the LSR, V_{tot} . The highest metallicity stars in the sample span essentially the same range of velocities as the solar-abundance and sub-solar abundance ESP host stars.

Several previous studies have commented on the relatively low velocity ($\sim 13 \text{ kms}^{-1}$) of the Sun with respect to the LSR. Gonzalez (1999), in particular, has invoked the Weak Anthropic Principle (Barrow & Tipler, 1988) in conjunction with this property, arguing that the small offset from co-rotation minimises excursions into the potentially dangerous environment (supernovae, gravitational interactions) of spiral arms, therefore providing the long term quiescence which may be necessary for advanced life forms to develop. We can make two points in this context:

- first, it is clear from Figure 12 than $\sim 10\%$ of the known ESP host stars have velocities, V_{tot} , within a few kms^{-1} of that of the Sun. Indeed, the transiting system, HD 209458, has a space motion with respect to the LSR which is almost identical with that of the Sun, while HD 114783 has a relative motion of only 6.2 kms^{-1} . Gonzalez *et al.* (2001) derive age estimates of 3 Gyrs (isochrones) and 4.3 Gyrs (activity) for the former star. HD 114783 is too red to allow reliable an isochrone-based age estimate, but Vogt *et al.* (2001) note that HD 114783 is chromospherically inactive, $\log R'_{HK} = -4.96$, or ~ 4.8 Gyrs for the Donahue (1993) calibration. Both stars are therefore likely to have ages similar to that of the Sun.
- second, the Weak Anthropic Principle (WAP) can be expressed in two ways: as a positive concept, in that the planetary environment must permit the development of

advanced lifeforms; or as a less restrictive, negative concept, in that the environment should not be inimical to the development of advanced lifeforms. Whether one chooses to express the WAP as a positive or a negative concept depends on other issues, notably belief in the likelihood of life developing elsewhere in the Universe. In either case, with a current sample of one known inhabited planet, the WAP should be given the same scientific weight as its converse, the Copernican Principle (“we’re not special”). Both are interesting philosophical concepts, which may have explanatory power; neither carries any evidentiary weight in the present context.

Finally, we have compared the distribution of properties of the extrasolar planetary systems against the systemic velocities to search for possible trends or correlations. The only potentially significant result is shown in the uppermost panel of Figure 13, plotting $M_2 \sin i$ against velocity perpendicular to the Plane. The data suggest that, with the exception of HD 114762, higher-mass companions tend to be found in systems with low W velocities. The result is statistically marginal, but might indicate a correlation with the mass of the parent circumstellar disk. Clearly more data are required to confirm whether this effect is real.

5. Summary and conclusions

Over sixty stars with planetary-mass companions are now known. While these stars neither constitute a volume-limited sample nor, probably, a complete sampling of the full range of planetary systems, they provide sufficient numbers for a preliminary investigation of the characteristics of the parent stars. In this paper we have compared the chemical abundance distribution and kinematics of those stars against data for representative samples of the local disk. Our metallicities are based on Strömgren photometry, using the calibration derived by Schuster & Nissen (1989). We have shown that the resulting metallicity scale is offset to lower abundances with respect to recent high-resolution spectroscopic measurements. This discrepancy is not important for our purposes, since Strömgren photometry is available for 86% of our reference sample - an Hipparcos-selected sample of 486 F, G and K stars within 25 parsecs of the Sun. The abundance distributions derived for both datasets are therefore internally consistent, although the solar abundance on this scale is $[Fe/H]_{uvby} \sim -0.1$ dex.

Comparing the abundance distributions of the two datasets, it is clear that, as noted in previous studies, systems currently known to have extrasolar planets are heavily weighted to high metallicities. We have used the fraction of known ESP systems in the volume-complete sample (20/486, or 4.1%) to set the two distributions on a common scaling, and compute the observed frequency as a function of chemical abundance. The results show a strong trend with abundance, with effectively 100% frequency at $[Fe/H]_{uvby} > 0.3$. However, even at

abundances of less than $\frac{1}{2}$ solar, 1 to 2% of stars are likely to have planetary-mass companions in the mass/semi-major axis/eccentricity range detectable using current techniques. Clearly, these statistics represent a lower limit to the actual frequency of extrasolar planetary systems.

How rare are solar-abundance F, G, and K stars with planets? Note that while the frequency of ESP hosts increases with $[\text{Fe}/\text{H}]$, the absolute number of systems declines rapidly at high abundances. Thus, planetary systems with parent stars of near-solar abundance contribute a significant fraction of the total current sample. Based on the full FGK25 Hipparcos dataset, the local number density of stars with metallicities within ± 0.15 dex of the solar abundance is $0.0044 \text{ stars pc}^{-3}$. The corresponding number density of ESP host stars, based on the data plotted in Figure 7, is $0.00018 \text{ stars pc}^{-3}$. Consider an annulus centred on the Solar Radius, $R_{\odot} = 8 \text{ kpc.}$, diameter 50 parsecs. Extrapolating from the local sample, we expect $\sim 17,500$ ESP host stars within this very limited subset of the Galactic Disk. Casting the net wider, consider a wedge, thickness (perpendicular to the Plane) 50 parsecs, between Galactic radii of 7 and 9 kiloparsecs, a range which encompasses relatively minor changes in mean abundance and stellar number density. Based on our calculations, we would expect a total of over 900,000 solar-type stars with Jovian-mass planetary companions.

We have also compared the kinematics of the ESP host stars against the local Galactic disk via observations of a volume-limited sample of M dwarfs. The planetary hosts exhibit a velocity distribution which is relatively well matched to a Gaussian in each component, but with lower dispersions than in the field-star sample. This suggests that the average age is only $\sim 60\%$ that of a representative subset of the disk. This may reflect the higher proportion of metal-rich stars in the ESP host sample. Individual stars, however, span a wide range of motions, with velocities of up to $50\text{-}60 \text{ kms}^{-1}$ with respect to the Local Standard of Rest, and no obvious correlation between kinematics and abundance.

I would like to thank Geoff Marcy for providing radial velocity measurements for several stars in advance of publication; David Trilling, for useful comments; and David Koerner, for interesting discussion and sparking my initial interest in this topic. The research for this paper made extensive use of the SIMBAD database, maintained by Strasberg Observatory, and of Jean Schneider's 'Extrasolar Planets Encyclopedia'.

REFERENCES

- Barrow, J.D., Tipler, F.J. 1988, *The Anthropic Cosmological Principle*, Oxford Univ. press (Oxford)

- Bessell, M.S. 2000, PASP, 112, 961
- Biemont, E., Baudoux, M., Kurucz, R.L, Ansbacher, W., Pinnington, E.H. 1991, A&A, 249, 539
- Butler, R.P., Vogt, S.S., Marcy, G.W., Fischer, D.A., Henry, G.W., Apps, K. 2000, ApJ, 545, 504
- Cayrel de Stobel, G., Soubiran, C., Friel, E.D., Ralite, N., Francois, P. 1997, A&AS, 124, 299
- Davis Philip, A.G., Egret, D. 1980, A&AS, 40, 199
- Dehnen, W., Binney, J.J. 1998, MNRAS, 298, 387
- Dick, S.J., 1998, *Life on other worlds*, Cambridge University Press, (Cambridge)
- Donahue, R.A., 1993, Ph.d. thesis, New Mexico State University
- Duflot, M., Figon, P. Meyssonier, N. 1995, A&AS, 114, 269
- ESA, 1997, The Hipparcos Catalogue
- Fabricius, C., Makarov, V.V. 2000, A&AS, 144, 45
- Favata, F., Micela, G., Sciortino, S. 1996, A&A, 311, 951
- Favata, F., Micela, G., Sciortino, S. 1997, A&A, 323, 809 (F97)
- Fouts, G., Sandage, A. 1986, AJ, 91, 1189
- Gatewood, G., Han, I., Black, D.C. 2001, ApJ, 548, L61
- Giménez, A. 2000, A&A, 356, 213
- Gizis, J.E., Reid, I.N., Hawley, S.L. 2001, AJ, subm. (PMSU3)
- Gliese, W. 1969, Catalogue of Nearby Stars, Veroff. Astr. Rechen-Instituts, Heidelberg, Nr. 22
- Gliese, W., Jahreiß, H. 1979, A&AS 38, 423
- Gonzalez, G. 1997, MNRAS, 285, 403
- Gonzalez, G. 1998, A&A, 334, 221

- Gonzalez, G. 1999, MNRAS, 308, 447
- Gonzalez, G., Vanture, A.D. 1998, A&A, 339, L29
- Gonzalez, G., Wallerstein, G., Saar, S. 1999, ApJ, 511, L111
- Gonzalez, G., Laws, C. 2000, AJ, 119, 390
- Gonzalez, G., Laws, C., Tyagi, S., Reddy, B.E. 2001, AJ, 121, 432
- Gratton, R.G., Carretta, E., Clementini, G., Sneden, C., 1997, in *Hipparcos Venice '97*, ed B Battrick (ESA), p 339
- Griffin, R.F. 1972, MNRAS, 155, 449
- Guillot, T. 1999, Science, 286, 272
- Halbwachs, J.L., Arenou, F., Mayor, M., Udry, S., Queloz, D. 2000, A&A, 355, 581
- Han, I., Black, D.C., Gatewood, G. 2001, ApJ, 548, L57
- Hauck, B., Mermilliod, M. 1998, A&AS, 129, 431
- Hawley, S.L., Gizis, J.E., Reid, I.N. 1996, AJ, 112, 2799 [PMSU2]
- Haywood, M. 2001, MNRAS, 325, 1365
- Heacox, W.D. 1999, ApJ, 526, 928
- Henry, T.J., Soderblom, D.R., Donahue, R.A., Baliunas, S.L. 1996, AJ, 111, 439
- Jahreiß, H., Wielen, R. 1997, Proc. ESA Stmp. 402, *Hipparcos - Venice '97*, ESA Publications, Noordwijk, p. 675
- Jorissen, A, Mayor, M., Udry, S. 2001, A&A, 379, 992
- Latham, D.W., Mazeh, T., Stefanik, R.P., Mayor, M., Burki, G. 1989, Nature, 339, 38
- Laughlin, G. 2000, ApJ, 545, 1064
- Laws, C., Gonzalez, G. 2001, ApJ, in press
- Lin, D.N.C., Bodenheimer, P., Richardson, D.C. 1996, Nature, 380, 606
- Lutz, T.E., Upgren A.R. 1980, AJ, 85, 573
- Mcgrath, M.A. *et al.* 2001, DPS, 33, 6001

- Marcy, G.W., Benitz, K.J. 1989, ApJ, 344, 441
- Marcy, G.W., Butler, R.P. 2000, PASP, 112, 137
- Mayor, M., Queloz, D. 1995, Nature, 378, 355
- Murray, N., Chaboyer, B., Arras, P., Hansen, B., Noyes, R.W. 2001, ApJ, 555, 810
- Murray, N., Chaboyer, B. 2001, ApJ, *subm.*
- Naef, D., Latham, D., Mayor, M. *et al.*, 2001, A&A, *in press*
- Nidever, D., Marcy, G.W., Butler, R.P., Fischer, D.A., Vogt, S.S. 2002, AJ, *subm.*
- Olsen, E.H. 1984, A&AS, 57, 443
- Oppenheimer, B.R., Hambly, N.C., Digby, A.P., Hodgkin, S.T., Saumon, D. 2001, Science, 292, 698
- Pourbaix, D. 2001, A&A, 369, L22
- Pourbaix, D., Arenou, F. 2001, A&A, 372, 935
- Randich, S., Gratton, R., Pallavicini, R., Pasquini, L., Carretta, E. 1999, A&A, 348, 487
- Reid, I.N., Hawley, S.L., Gizis, J.E. 1995, AJ, 110, 1838 [PMSU1]
- Reid, I.N. 1998 AJ, 115, 204
- Reid, I.N., Hawley, S.L., Gizis, J.E. 2002, AJ, *subm.* [PMSU4]
- Reid, I.N., Sahu, K.C., Hawley, S.L. 2001, ApJ, 559, 942
- Ryan, S.G. 1992, AJ, 104, 1144
- Santos, N.C., Israelian, G., Mayor, M. 2000, A&A, 363, 228
- Santos, N.C., Israelian, G., Mayor, M. 2001, A&A, 373, 1019
- Sargent, A.I., Beckwith, S.V.W. 1993, Physics Today, 46, 22
- Schaller, G., Schaerer, D., Meynet, G., Maeder, A. 1992, A&AS, 96, 269
- Schaerer, D., Charbonnel, C., Meynet, G., Maeder, A., Schaller, G. 1993, A&AS, 102, 339
- Schuster, W.J., Nissen, P.F. 1989, A&A, 221, 65

- Soderblom, D.R., Duncan, D.K., Johnson, D.R.H. 1991, ApJ, 375, 722
- Spitzer, L., Schwarzschild, M. 1953, ApJ, 118, 106
- Stepinski, T.F., Black, D.C. 2000, A&A, 356, 903
- Strömberg, B. 1966, Ann. Rev. Astr. Ap., 4, 433
- Tabachnik, S., Tremaine, S. 2001, AJ, in press
- Tinney, C.G., Butler, R.P., Marcy, G.W., Jones, H.R.A., Penny, A.J., Vogt, S.S., Apps, K., Henry, G.W. 2001. ApJ, 551, 507
- Vogt, S.S., Butler, R.P, Marcy, G.W., Fischer, D.A., Pourbaix, D., Apps, K., Laughlin, G. 2001a, ApJ, subm.
- Vogt, S.S., Butler, R.P, Marcy, G.W., Apps, K. 2001b, ApJ, in press
- Wielen, R. 1977, A&A, 60, 263
- Zucker, S., Mazeh, T. 2001, ApJ, 562, 1038
- S. Zucker, D. Naef, D.W. Latham, M. Mayor, T. Mazeh, *et al.* 2001, ApJ, in press

Table 1. The host stars

HIP	Name	M_V	(B-V)	π mas	$M_2 \sin i$ M_J	$a \sin i$ AU	P days	e	Comments
...	BD -10 3166	5.5:	0.84	12 ± 4	0.48	0.05	3.49	0.00	1
522	HD 142	3.65	0.52	39.00 ± 0.64	1.36	0.98	338.00	0.37	
1292	HD 1237	5.36	0.75	56.76 ± 0.53	3.31	0.49	133.82	0.51	
3479	HD 4208	5.21	0.67	30.58 ± 1.08	0.80	1.70	829.00	0.04	
3502	HD 4203	4.22	0.73	12.85 ± 1.27	1.64	1.09	406.00	0.53	1, subgiant
5054	HD 6434	4.69	0.60	24.80 ± 0.89	0.48	0.15	22.09	0.30	
6643	HD 8574	3.90	0.58	22.65 ± 0.82	2.23	0.76	228.80	0.40	
7513	HD 9826	3.44	0.54	74.25 ± 0.72	0.71	0.06	4.62	0.03	ν And, 2
8159	HD 10697	3.73	0.67	30.71 ± 0.81	6.59	2.00	1083.00	0.12	subgiant
9683	HD 12661	4.59	0.72	26.91 ± 0.83	2.83	0.78	264.50	0.33	
10138	HD 13445	5.98	0.77	91.63 ± 0.61	4.00	0.11	15.78	0.05	
12048	HD 16141	4.00	0.71	27.85 ± 1.39	0.21	0.35	75.82	0.28	subgiant
12653	HD 17051	4.22	0.57	58.00 ± 0.55	2.26	0.92	320.10	0.16	ι Hor
14954	HD 19994	3.31	0.57	44.69 ± 0.75	2.00	1.30	454.00	0.20	
16537	HD 22049	6.19	0.88	310.74 ± 0.85	0.86	3.30	2502.10	0.61	ϵ Eri
17096	HD 23079	4.42	0.58	28.90 ± 0.56	2.54	1.48	627.30	0.06	
19921	HD 27442	3.14	1.08	54.84 ± 0.50	1.43	1.18	423.00	0.02	subgiant
20723	HD 28185	4.82	0.71	25.28 ± 1.08	5.60	1.00	385.00	0.06	
24205	HD 33636	4.77	0.58	34.85 ± 1.33	7.70	2.60	1553.00	0.39	
26381	HD 37124	5.07	0.67	30.08 ± 1.15	1.04	0.58	155.00	0.19	
26394	HD 39091	4.35	0.60	54.92 ± 0.45	10.37	3.34	2115.30	0.62	
27253	HD 38529	2.80	0.74	23.57 ± 0.92	0.81	0.13	14.41	0.28	subgiant
31246	HD 46375	5.22	0.86	29.93 ± 1.07	0.25	0.04	3.02	0.02	
33212	HD 50554	4.40	0.53	32.23 ± 1.01	4.90	2.38	1279.00	0.42	
33719	HD 52265	4.06	0.54	35.63 ± 0.84	1.13	0.49	118.96	0.29	
40687	HD 68988	4.36	0.62	17.00 ± 0.96	1.90	0.07	6.28	0.14	
42723	HD 74156	3.57	0.54	15.49 ± 1.01	1.56	0.28	51.61	0.65	3
43177	HD 75289	4.05	0.58	34.55 ± 0.56	0.42	0.05	3.51	0.00	
43587	HD 75732	5.46	0.87	79.80 ± 0.84	0.84	0.11	14.65	0.05	55 Cnc
45982	HD 80606	5.10	0.72	17.13 ± 5.77	3.41	0.44	111.78	0.93	

Table 1—Continued

HIP	Name	M_V	(B-V)	π mas	$M_2 \sin i$ M_J	$a \sin i$ AU	P days	e	Comments
47007	HD 82943	4.35	0.59	36.42 ± 0.84	0.88	0.73	221.60	0.54	4
47202	HD 83443	5.05	0.79	22.97 ± 0.90	0.35	0.04	2.99	0.08	5
50786	HD 89744	2.79	0.49	25.65 ± 0.70	7.20	0.88	256.00	0.70	
52409	HD 92788	4.76	0.69	30.94 ± 0.99	3.80	0.94	340.00	0.36	
53721	HD 95128	4.36	0.56	71.04 ± 0.66	2.41	2.10	1096.00	0.10	47 UMa, 6
59610	HD 106252	4.49	0.64	26.71 ± 0.91	6.81	2.61	1500.00	0.54	
60644	HD 108147	4.07	0.50	25.93 ± 0.69	0.34	0.10	10.88	0.56	
64426	HD 114762	4.26	0.52	24.65 ± 1.44	11.00	0.30	84.03	0.33	7
64457	HD 114783	6.02	0.91	48.95 ± 1.06	0.99	1.20	501.00	0.10	
65721	HD 117176	3.71	0.69	55.22 ± 0.73	6.60	0.43	116.60	0.40	70 Vir, subgiant
67275	HD 120136	3.53	0.48	64.12 ± 0.70	3.87	0.05	3.31	0.02	τ Boo
68162	HD 121504	4.30	0.59	22.54 ± 0.91	0.89	0.32	64.60	0.13	
72339	HD 130332	5.68	0.75	33.60 ± 1.51	1.08	0.09	10.72	0.05	
74500	HD 134987	4.40	0.70	38.98 ± 0.98	1.58	0.78	260.00	0.25	
77740	HD 141937	4.63	0.60	29.89 ± 1.08	9.70	1.49	658.80	0.40	
78459	HD 143761	4.19	0.61	57.38 ± 0.71	1.10	0.23	39.47	0.03	ρ CrB
79248	HD 145675	5.38	0.90	55.11 ± 0.59	3.30	2.50	1619.00	0.35	14 Her
86796	HD 160691	4.23	0.70	65.46 ± 0.80	1.97	1.65	743.00	0.62	subgiant
87330	HD 162020	6.63	0.96	31.99 ± 1.48	13.73	0.08	8.43	0.28	
89844	HD 168443	4.03	0.70	26.40 ± 0.85	7.20	0.29	57.90	0.54	8, subgiant
90004	HD 168746	4.78	0.69	23.19 ± 0.96	0.24	0.07	6.41	0.00	
90485	HD 169830	3.11	0.48	27.53 ± 0.91	2.96	0.82	230.40	0.34	
93746	HD 177830	3.32	1.09	16.94 ± 0.76	1.28	1.00	391.00	0.43	subgiant
94076	HD 178911	3.29	0.63	20.42 ± 1.57	6.29	0.33	71.49	0.12	subgiant
94645	HD 179949	4.09	0.51	36.97 ± 0.80	0.84	0.05	3.09	0.05	
96901	HD 186427	4.55	0.66	46.70 ± 0.52	1.50	1.70	804.00	0.67	16 CygB
97336	HD 187123	4.46	0.61	20.87 ± 0.71	0.52	0.04	3.10	0.03	
98714	HD 190228	3.34	0.75	16.10 ± 0.81	4.99	2.31	1127.00	0.43	subgiant
99711	HD 192263	6.30	0.94	50.27 ± 1.23	0.76	0.15	23.87	0.03	
100970	HD 195019	4.05	0.64	26.77 ± 0.89	3.43	0.14	18.30	0.05	

Table 1—Continued

HIP	Name	M_V	(B-V)	π mas	$M_2 \sin i$ M_J	$a \sin i$ AU	P days	e	Comments
104903	HD 202206	4.75	0.71	21.58 ± 1.14	14.68	0.80	258.97	0.42	
108859	HD 209458	4.29	0.53	21.24 ± 1.00	0.69	0.05	3.53	0.00	
109378	HD 210277	4.90	0.77	46.97 ± 0.79	1.28	1.10	437.00	0.45	
111143	HD 213240	3.75	0.61	24.54 ± 0.81	3.70	1.60	759.00	0.31	
113020	Gl 876	11.81	1.60	212.69 ± 2.10	1.98	0.21	61.02	0.27	9
113357	HD 217014	4.56	0.66	65.10 ± 0.76	0.47	0.05	4.23	0.00	51 Peg
113421	HD 217107	4.71	0.72	50.71 ± 0.75	1.28	0.07	7.11	0.14	
116906	HD 222582	4.59	0.60	23.84 ± 1.11	5.40	1.35	576.00	0.71	

Note. — Column 1 lists the Hipparcos designation, where appropriate; column 2 gives the common name; columns 3 and 4 list M_V and (B-V), generally derived from the literature data listed in the Hipparcos catalogue; column 5 lists the parallax and associated uncertainty (in milliarcseconds); column 6, 7, 8 and 9 list the mass, semi-major axis, period and eccentricity of the planetary-mass companions. The latter data are taken from J. Schneider’s on-line catalogue (<http://cfa-www.harvard.edu/planets/catalog.html>), except for HD 162020 and HD 202206, where the data are from the Geneva Observatory web-site (<http://obswww.unige.ch/udry/planet/>). Named stars, evolved stars and stars with more than one companion (see below) are identified in the final column.

Notes for individual stars:

1. Selected for monitoring based on high metallicity (Butler *et al.*, 2000)
2. At least 2 other planetary-mass companions, $M \sin i = 2.11, 4.61 M_J$ at $a \sin i = 0.83, 2.50$ AU
3. At least 1 other planet/brown dwarf companion, $M \sin i = 7.5 M_J$ at $a \sin i = 4.47$ AU
4. At least 1 other planet companion, $M \sin i = 1.63 M_J$ at $a \sin i = 1.16$ AU
5. At least 1 other planet companion, $M \sin i = 0.16 M_J$ at $a \sin i = 0.174$ AU
6. At least 1 other planet companion, $M \sin i = 0.76 M_J$ at $a \sin i = 3.73$ AU
7. Suspected high inclination, implying brown dwarf companion
8. At least 1 other planet/brown dwarf companion, $M \sin i = 17.1 M_J$ at $a \sin i = 2.87$ AU
9. At least 1 other planet companion, $M \sin i = 0.56 M_J$ at $a \sin i = 0.13$ AU

Table 2. Strömgren data and abundance measurements

HIP	$[\text{Fe}/\text{H}]_{sp}$	ref.	(b-y)	m_1	c_1	$[\text{Fe}/\text{H}]_{uvby}$	$\delta[\text{Fe}/\text{H}]$
522	0.04	10	0.332	0.168	0.416	-0.06	-0.10
1292	0.11	1	0.459	0.289	0.300	-0.06	-0.17
3479	-0.24	9	0.413	0.213	0.285	-0.22	0.02
3502	0.22	9	0.467	0.288	0.392	0.22	0.00
5054	-0.55	1	0.384	0.159	0.274	-0.54	0.01
6643	-0.09	11	0.362	0.169	0.378	-0.22	-0.13
7513	0.12	2	0.346	0.176	0.415	-0.02	-0.14
8159	0.16	3	0.440	0.238	0.379	0.08	-0.08
9683	0.35	3	0.448	0.267	0.398	0.25	-0.10
10138	-0.20	1	0.484	0.337	0.287	-0.14	0.06
12048	0.15	1	0.422	0.213	0.378	-0.02	-0.17
12653	0.25	1	0.357	0.188	0.364	0.08	-0.17
14594	0.26	1	0.361	0.185	0.422	0.00	-0.26
16537	-0.07	1	0.504	0.430	0.263	-0.28	-0.21
17096	...		0.369	0.179	0.330	-0.14	
19921	0.22	12	0.651	0.513	0.406	0.26	0.04
20723	0.24	1	0.443	0.264	0.352	0.15	-0.09
24205	-0.13	9	0.378	0.177	0.324	-0.20	-0.07
26381	-0.41	3	0.421	0.202	0.280	-0.37	0.04
26394	...		0.371	0.193	0.363	0.09	
27253	0.39	1	0.471	0.278	0.437	0.23	-0.16
31246	0.21	3	0.502	0.401	0.337	0.01	-0.20
33212	0.02	11	0.366	0.179	0.347	-0.12	-0.14
33719	0.24	1	0.360	0.190	0.404	0.08	-0.16
40687	0.24	9	0.405	0.244	0.387	0.36	0.12
42723	0.13	11	0.375	0.181	0.390	-0.06	-0.19
43177	0.27	1	0.360	0.191	0.405	0.10	-0.17
43587	0.45	4	0.536	0.357	0.415	0.10	-0.35
45982	0.43	5	0.470	0.312	0.361	0.20	-0.23
47007	0.33	1	0.386	0.217	0.390	0.27	-0.06
47202	0.39	1	0.488	0.349	0.368	0.18	-0.21

Table 2—Continued

HIP	$[\text{Fe}/\text{H}]_{sp}$	ref.	(b-y)	m_1	c_1	$[\text{Fe}/\text{H}]_{uvby}$	$\delta[\text{Fe}/\text{H}]$
50786	0.30	3	0.338	0.184	0.451	0.14	-0.16
52409	0.31	3	0.433	0.253	0.376	0.22	-0.09
53721	0.01	6	0.391	0.202	0.343	0.02	0.01
59610	-0.16	11	0.390	0.187	0.341	-0.13	0.03
60644	0.20	1	0.346	0.177	0.391	-0.01	-0.21
64426	-0.60	6	0.365	0.125	0.297	-0.74	-0.14
64457	0.33	9	0.521	0.458	0.309	-0.17	-0.50
65721	-0.01	6	0.446	0.232	0.351	-0.07	-0.06
67275	0.32	7	0.318	0.177	0.439	0.13	-0.19
68162	0.17	1	0.381	0.189	0.361	-0.02	-0.19
72339	0.05	3	0.475	0.305	0.316	-0.02	-0.07
74500	0.32	3	0.435	0.256	0.374	0.22	-0.10
77740	0.16	11	0.388	0.225	0.346	0.24	0.08
78459	-0.29	6	0.394	0.178	0.337	-0.27	0.02
79248	0.50	8	0.537	0.366	0.438	0.13	-0.37
86796	0.28	10	0.432	0.244	0.393	0.20	-0.08
87330	0.01	1	0.579	0.534	0.244	0.11	0.10
89844	0.10	3	0.455	0.233	0.377	-0.06	-0.16
90004	-0.06	1	0.435	0.223	0.342	-0.09	-0.03
90485	0.22	1	0.328	0.177	0.446	0.09	-0.13
94076	0.28	13	0.403	0.219	0.378	0.16	-0.12
94645	0.22	14	0.346	0.183	0.384	0.08	-0.14
96901	0.07	7	0.416	0.226	0.354	0.09	0.02
97336	0.16	8	0.405	0.224	0.365	0.17	0.01
98714	-0.24	1	0.482	0.264	0.306	-0.27	-0.03
99711	-0.03	3	0.541	0.493	0.275	-0.20	-0.17
100970	0.16	15	0.419	0.204	0.362	-0.11	-0.27
104903	0.37	1	0.435	0.253	0.390	0.24	-0.13
108859	0.04	3	0.361	0.174	0.362	-0.15	-0.19
109378	0.23	1	0.466	0.285	0.369	0.16	-0.07
111143	0.16	1	0.387	0.190	0.399	-0.02	-0.18

Table 2—Continued

HIP	[Fe/H] _{sp}	ref.	(b-y)	m ₁	c ₁	[Fe/H] _{uvby}	δ[Fe/H]
113357	0.21	3	0.416	0.233	0.371	0.18	-0.03
113421	0.39	1	0.456	0.299	0.376	0.28	-0.11
116906	-0.01	16	0.406	0.202	0.345	-0.08	-0.07

Note. — Column 2 lists abundances derived from high-resolution spectroscopy from the following sources:

1. Santos *et al.*, 2001; 2. Gonzalez & Laws, 2000; 3. Gonzalez *et al.*, 2001; 4. Gonzalez & Vanture, 1998; 5. Naef *et al.*, 2001; 6. Gonzalez, 1998; 7. Laws & Gonzalez, 2001; 8. Gonzalez *et al.*, 1999; 9. Vogt *et al.*, 2001a; 10. Favata *et al.*, 1997; 11. Geneva Observatory (<http://obswww.unige.ch/udry/planet/>); 12. Randich *et al.*, 1999; 13. Zucker *et al.*, 2001; 14. Tinney *et al.*, 2001; 15. Santos *et al.*, 2000; 16. Vogt *et al.*, 2001b.

Columns 4, 5 and 6 list Strömgren (b-y), m₁ and c₁ data from Hauck & Mermilliod (1998), and Column 7 lists [Fe/H] derived from those data using the Schüster & Nissen (1989) calibration.

Column 8 lists $\delta[\text{Fe}/\text{H}] = [\text{Fe}/\text{H}]_{uvby} - [\text{Fe}/\text{H}]_{sp}$.

Table 3. Space motions

HIP	π mas	μ_α mas	μ_δ mas	V_{rad} kms ⁻¹	ref.	U kms ⁻¹	V kms ⁻¹	W kms ⁻¹	V_{LSR} kms ⁻¹	Comments
522	39.00 ± 0.64	575.2	-39.9	2.6	2	-58.2	-37.2	-12.1	58.0	
1292	56.76 ± 0.53	433.9	-57.9	-5.8	1	-33.0	-16.6	2.7	27.5	
3479	30.58 ± 1.08	313.5	150.0	55.4	2	-53.1	-5.2	-55.9	65.0	
3502	12.85 ± 1.27	125.2	-124.0	-14.1	7	-16.5	-59.3	-25.2	57.3	
5054	24.80 ± 0.89	-169.0	-527.7	23.0	1	85.4	-66.6	-3.4	113.5	
6643	22.65 ± 0.82	252.6	-158.6	18.9	1	-44.3	-37.0	-30.3	52.1	
7513	74.25 ± 0.72	-172.6	-381.0	-28.3	2	28.5	-22.1	-14.6	42.7	
8159	30.71 ± 0.81	-45.0	-105.4	-43.5	1	35.6	-26.7	15.0	55.0	
9683	26.91 ± 0.83	-107.8	-175.3	-52.2	6	55.1	-31.7	-0.1	70.6	
10138	91.63 ± 0.61	2092.8	654.5	56.6	1	-97.5	-75.9	-28.5	114.4	
12048	27.85 ± 1.39	-156.9	-437.1	-53.0	2	85.8	-41.0	2.4	102.7	
12653	58.00 ± 0.55	333.7	219.2	15.5	2	-31.2	-16.7	-7.3	24.1	
14594	44.69 ± 0.75	-209.6	-69.2	18.3	2	2.9	9.0	-28.2	28.5	
16537	310.74 ± 0.85	-976.4	18.0	15.5	2	-3.3	7.2	-20.0	19.1	
17096	28.90 ± 0.56	-193.6	-91.9	-22.2	8	29.1	29.6	1.4	53.2	
19921	54.84 ± 0.50	-48.0	-167.8	29.3	2	15.1	-22.1	-19.3	32.5	
20723	25.28 ± 1.08	80.8	-31.1	50.3	1	-49.2	-15.2	-11.7	40.7	
24205	34.85 ± 1.33	180.8	-137.3	-1.0	6	5.8	-28.2	11.1	33.3	
26381	30.08 ± 1.15	-79.8	-420.0	-12.0	2	21.6	-47.4	-44.4	64.4	
26394	54.92 ± 0.45	312.0	1050.2	9.4	2	-82.9	-46.4	0.5	84.1	
27253	23.57 ± 0.92	-80.1	-141.8	28.9	2	-12.6	-24.8	-33.7	33.0	
31246	29.93 ± 1.07	114.2	-96.8	4.0	2	6.0	-21.5	8.8	27.9	
33212	32.23 ± 1.01	-37.3	-96.4	-3.9	1	3.6	-10.0	-11.5	15.0	
33719	35.63 ± 0.84	-115.8	80.3	53.8	1	-52.2	-21.0	-8.7	45.1	
40687	17.00 ± 0.96	128.3	31.7	-69.5	7	75.1	-21.0	-10.6	86.6	
42723	15.49 ± 1.01	25.0	-200.5	3.8	1	28.8	-51.7	-18.4	61.5	
43177	34.55 ± 0.56	-20.5	-227.7	9.3	1	20.9	-12.5	-21.8	34.9	
43587	79.80 ± 0.84	-485.5	-234.4	26.6	2	-36.5	-18.2	-8.1	29.5	
45982	17.13 ± 5.77	47.0	6.9	3.8	1	6.9	2.9	11.4	26.5	
47007	36.42 ± 0.84	2.4	-174.1	8.1	1	10.3	-19.8	-8.9	25.0	

Table 3—Continued

HIP	π mas	μ_α mas	μ_δ mas	V_{rad} kms $^{-1}$	ref.	U kms $^{-1}$	V kms $^{-1}$	W kms $^{-1}$	V_{LSR} kms $^{-1}$	Comments
47202	22.97 \pm 0.90	22.4	-120.8	28.8	1	20.0	-30.4	-12.1	39.4	
50786	25.65 \pm 0.70	-120.2	-138.6	-6.5	2	-10.5	-29.7	-14.1	25.4	
52409	30.94 \pm 0.99	-12.6	-222.8	-4.5	1	16.1	-22.2	-20.9	34.0	
53721	71.04 \pm 0.66	-315.9	55.2	12.6	2	-24.6	-2.6	2.1	17.5	
59610	26.71 \pm 0.91	23.8	-279.4	15.5	1	28.8	-43.4	0.3	54.9	
60644	25.93 \pm 0.69	-181.6	-60.8	-5.1	1	-30.4	-11.6	-13.9	22.4	
64426	24.65 \pm 1.44	-582.7	-2.0	49.9	2	-81.8	-69.9	59.0	117.0	
64457	48.95 \pm 1.06	-138.1	9.6	-12.0	7	-15.5	-2.8	-8.7	6.2	
65721	55.22 \pm 0.73	-234.8	-576.2	4.9	2	13.3	-51.8	-4.0	52.1	
67275	64.12 \pm 0.70	-480.3	54.2	-15.6	2	-33.5	-19.0	-6.3	27.2	
68162	22.54 \pm 0.91	-250.6	-84.0	19.5	1	-27.6	-52.0	-1.4	50.3	
72339	33.60 \pm 1.51	-129.6	-140.8	-12.5	1	-9.3	-26.2	-10.7	21.2	
74500	38.98 \pm 0.98	-399.0	-75.1	3.4	2	-21.6	-39.6	20.3	45.5	
77740	29.89 \pm 1.08	97.1	24.0	-3.0	1	2.8	13.3	-8.7	22.6	
78459	57.38 \pm 0.71	-196.9	-773.0	18.4	2	54.7	-35.4	20.8	76.7	
79248	55.11 \pm 0.59	132.5	-298.4	-13.9	1	23.8	-12.2	-16.3	35.6	
86796	65.46 \pm 0.80	-15.1	-191.2	9.0	2	2.9	-14.4	-7.6	15.8	
87330	31.99 \pm 1.48	21.0	-25.2	-27.5	1	-27.7	2.7	-1.0	20.4	
89844	26.40 \pm 0.85	-92.2	-224.2	-48.7	1	-29.7	-57.9	-6.1	56.2	
90004	23.19 \pm 0.96	-22.1	-69.2	-25.6	1	-19.4	-22.3	-2.9	19.8	
90485	27.53 \pm 0.91	-0.8	15.2	-17.2	1	-16.9	1.1	4.0	14.6	
93746	16.94 \pm 0.76	-40.7	-51.8	-74.0	2	-23.8	-72.1	-7.0	68.2	
94076	20.42 \pm 1.57	47.1	194.5	-40.4	1	-58.3	-19.7	1.4	51.2	
94645	36.97 \pm 0.80	114.8	-101.8	-24.7	7	-26.6	-12.9	-11.0	18.7	
96901	46.70 \pm 0.52	-135.1	-163.5	-27.1	2	17.8	-29.6	-1.7	37.4	
97336	20.87 \pm 0.71	143.1	-123.2	-17.5	3	2.3	-16.0	-43.4	39.7	
98714	16.10 \pm 0.81	104.9	-69.8	-50.2	1	-20.0	-47.3	-35.6	51.6	
99711	50.27 \pm 1.23	-63.4	262.3	-10.8	1	-16.4	10.1	19.8	31.8	
100970	26.77 \pm 0.89	349.5	-56.9	-92.7	2	-72.3	-77.3	-36.5	99.6	
104903	21.58 \pm 1.14	-38.2	-119.8	14.6	1	22.5	-19.2	-10.0	35.5	

Table 3—Continued

HIP	π mas	μ_α mas	μ_δ mas	V_{rad} kms ⁻¹	ref.	U kms ⁻¹	V kms ⁻¹	W kms ⁻¹	V_{LSR} kms ⁻¹	Comments
108859	21.24 ± 1.00	28.9	-18.4	-14.8	1	-5.6	-15.6	0.6	13.7	
109378	46.97 ± 0.79	85.5	-449.8	-20.9	3	4.3	-50.2	-6.2	47.1	
111143	24.54 ± 0.81	-135.2	-194.1	-0.5	1	25.6	-29.9	23.1	52.9	
113020	212.69 ± 2.10	960.3	-675.6	-1.8	5	-12.5	-20.0	-11.5	15.5	
113357	65.10 ± 0.76	208.1	61.0	-31.2	2	-14.9	-28.0	14.7	31.9	
113421	50.71 ± 0.75	-6.1	-16.0	-12.1	4	-1.1	-7.8	9.3	19.0	
116906	23.84 ± 1.11	-145.4	-111.1	12.1	7	36.6	-0.3	-11.5	46.4	

Note. — Columns 2, 3 and 4 list astrometric data from the Hipparcos catalogue; column 5 shows the measured radial velocity and column 6 gives the source, as follows:

1. Geneva Observatory (<http://obswww.unige.ch/udry/planet/>) - measurements accurate to 1-10 ms⁻¹
2. the compilation by Dufloc *et al.*, 1995 - measurements accurate to 2-5 kms⁻¹
3. Marcy, as cited in Gonzalez (1999)
4. Griffin, 1972 - accurate to 0.4 kms⁻¹
5. Marcy & Benitz, 1989 - accurate to 0.3 kms⁻¹
6. Fouts & Sandage, 1986
7. Nidever *et al.* (2002)
8. Marcy (2001), priv. comm.

Columns 7, 8 and 9 list the space motions, and column 10 gives the velocity with respect to the Local Standard of Rest.

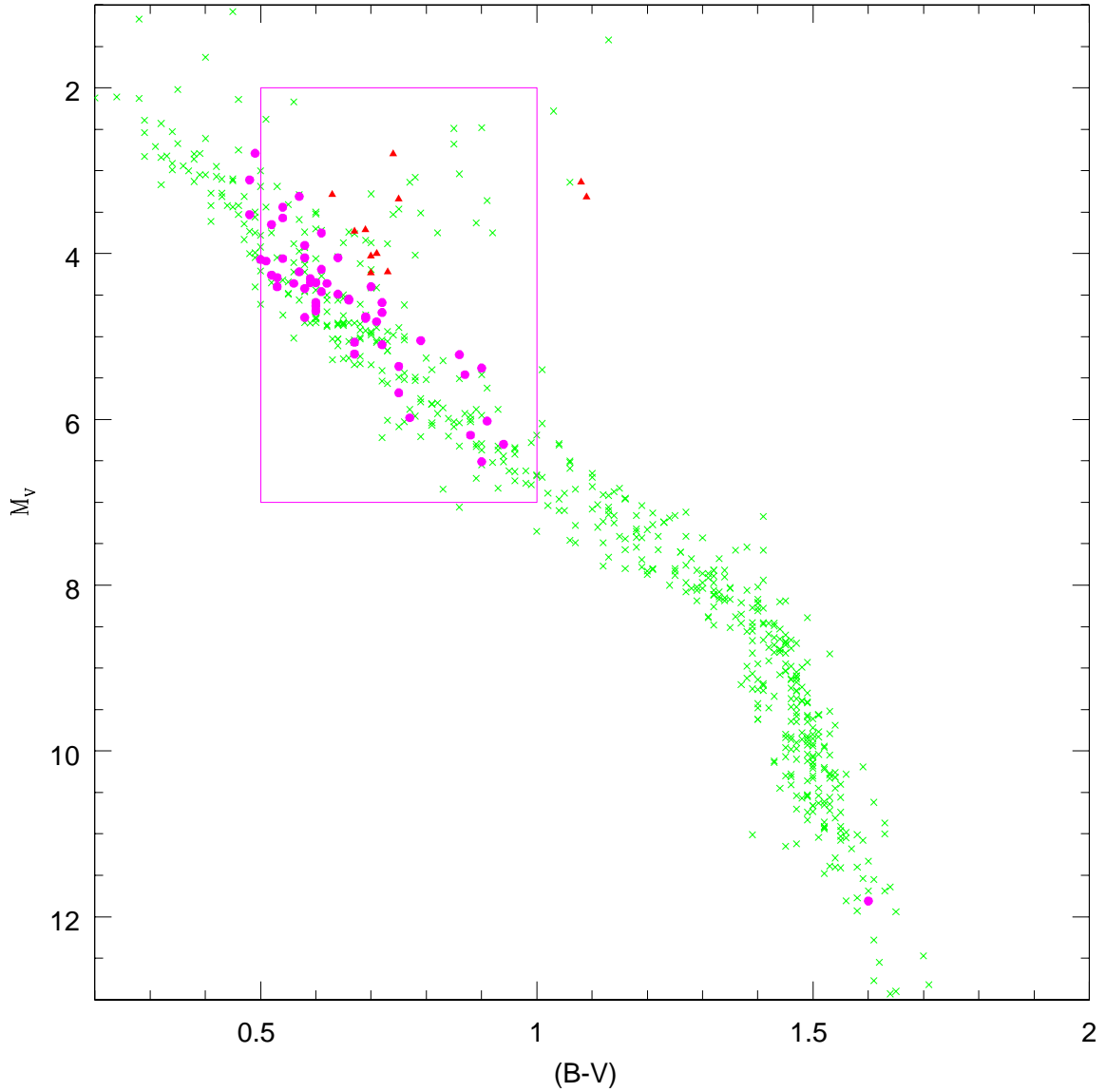


Fig. 1.— The location of the host stars of planets in the $(M_V, (B-V))$ diagram. The main-sequence is defined by stars with trigonometric parallaxes measured to an accuracy of better than 10%; main-sequence planetary hosts are plotted as solid points, evolved stars are plotted as solid triangles. The box marks the location of the reference sample (see Figure 4).

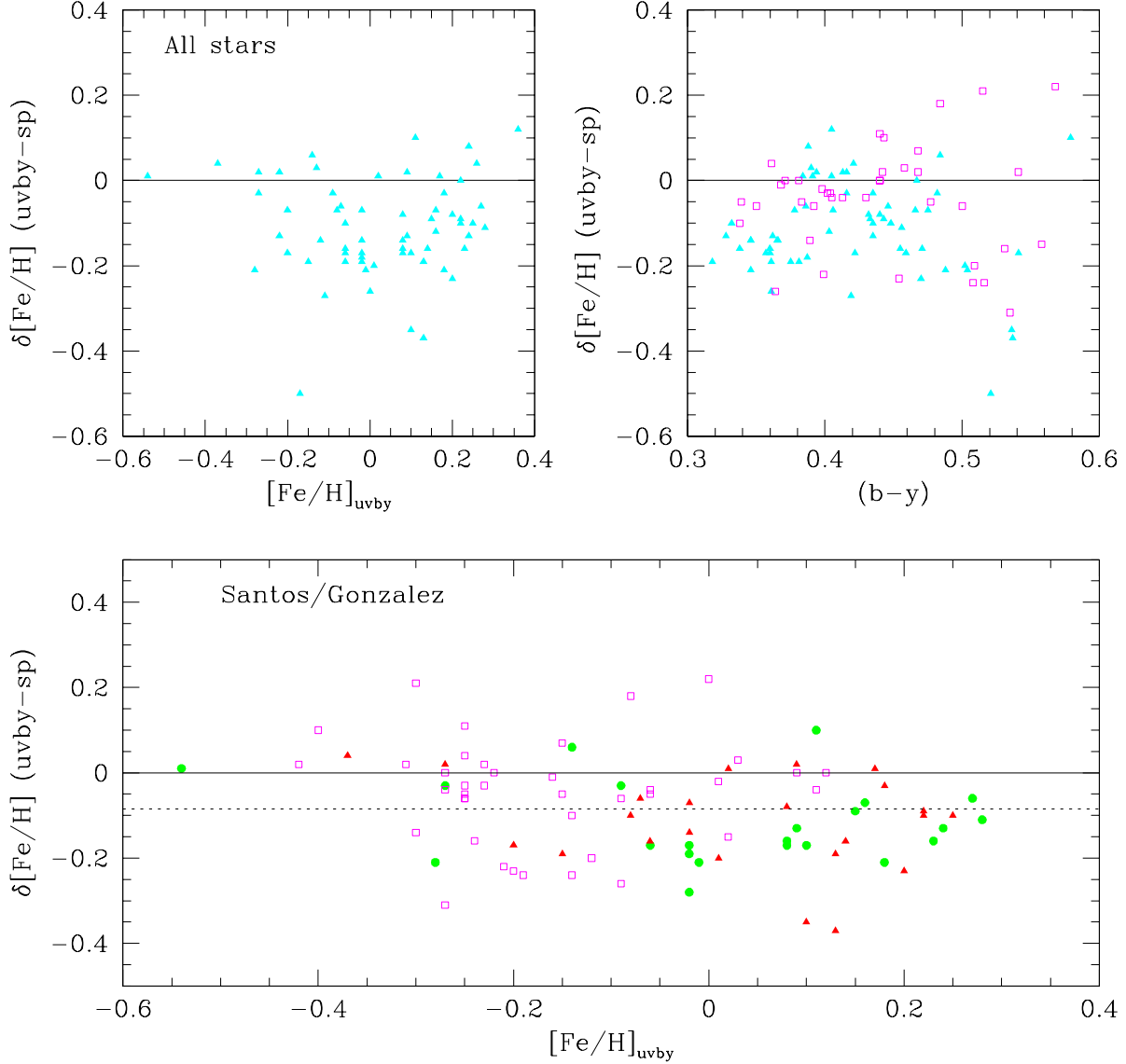


Fig. 2.— Comparison between spectroscopic and Strömgren-based abundance estimates for stars known to have planets. The upper two panels plot the data given in Table 2 as solid triangles, with field stars from Santos *et al.* (2001) plotted as open squares in the upper right panel. The lower panel plots data from Santos *et al.* (2001: solid points) and from the various analyses by Gonzalez and collaborators (solid triangles). Data for field stars analysed by Santos *et al.* are plotted as open squares. The dotted line marks the mean offset between these abundance calibrations.

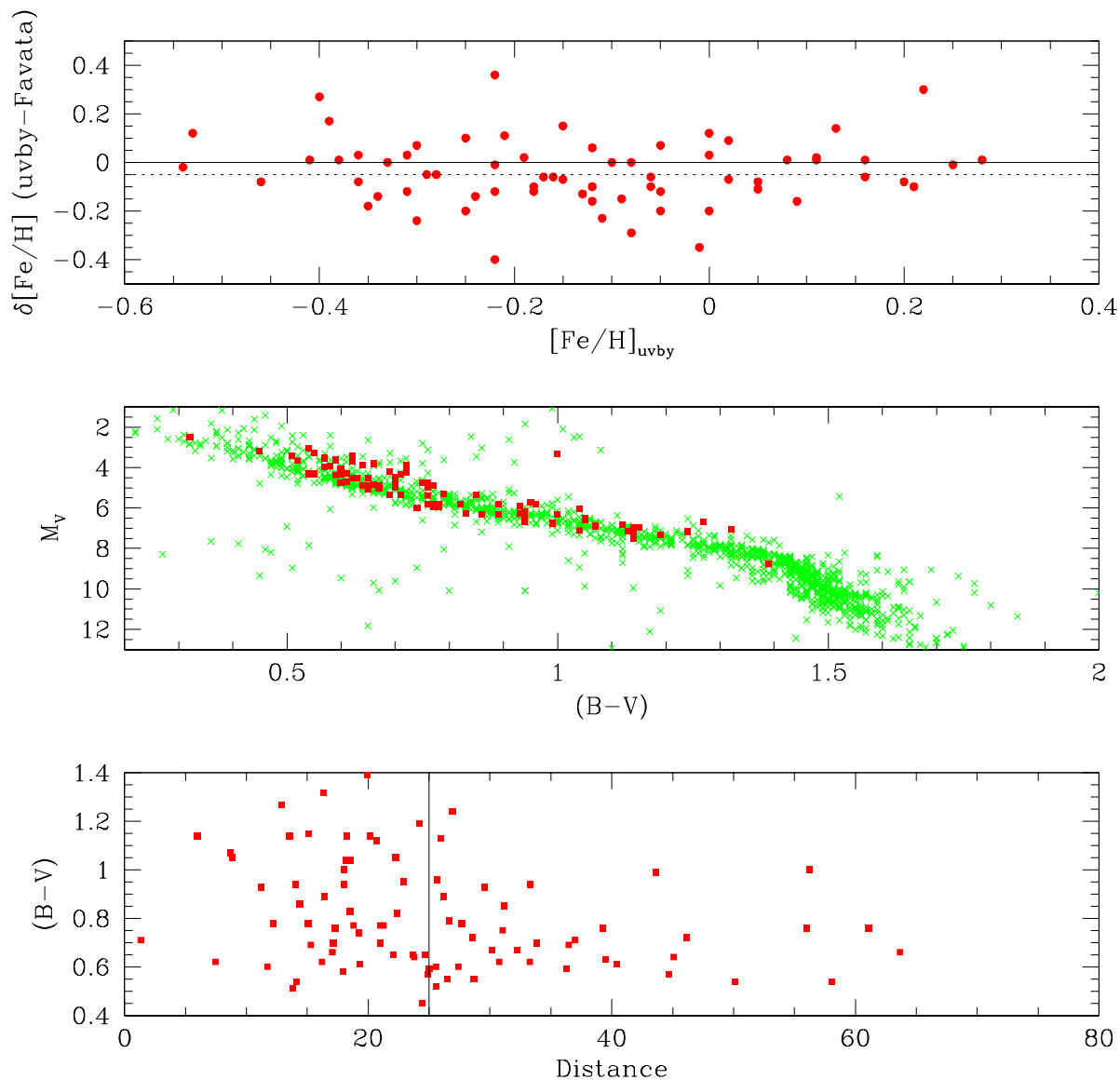


Fig. 3.— Data for stars in the Favata *et al.* (1997) disk dwarf sample. The upper panel compares the abundances against the Strömgren calibration, with the dotted line marking the mean offset. The middle panel shows the distribution in the HR diagram, where the solid squares mark the F97 stars. The lower panel plots the distance distribution, with the vertical line marking the nominal distance limit of the Gliese catalogue.

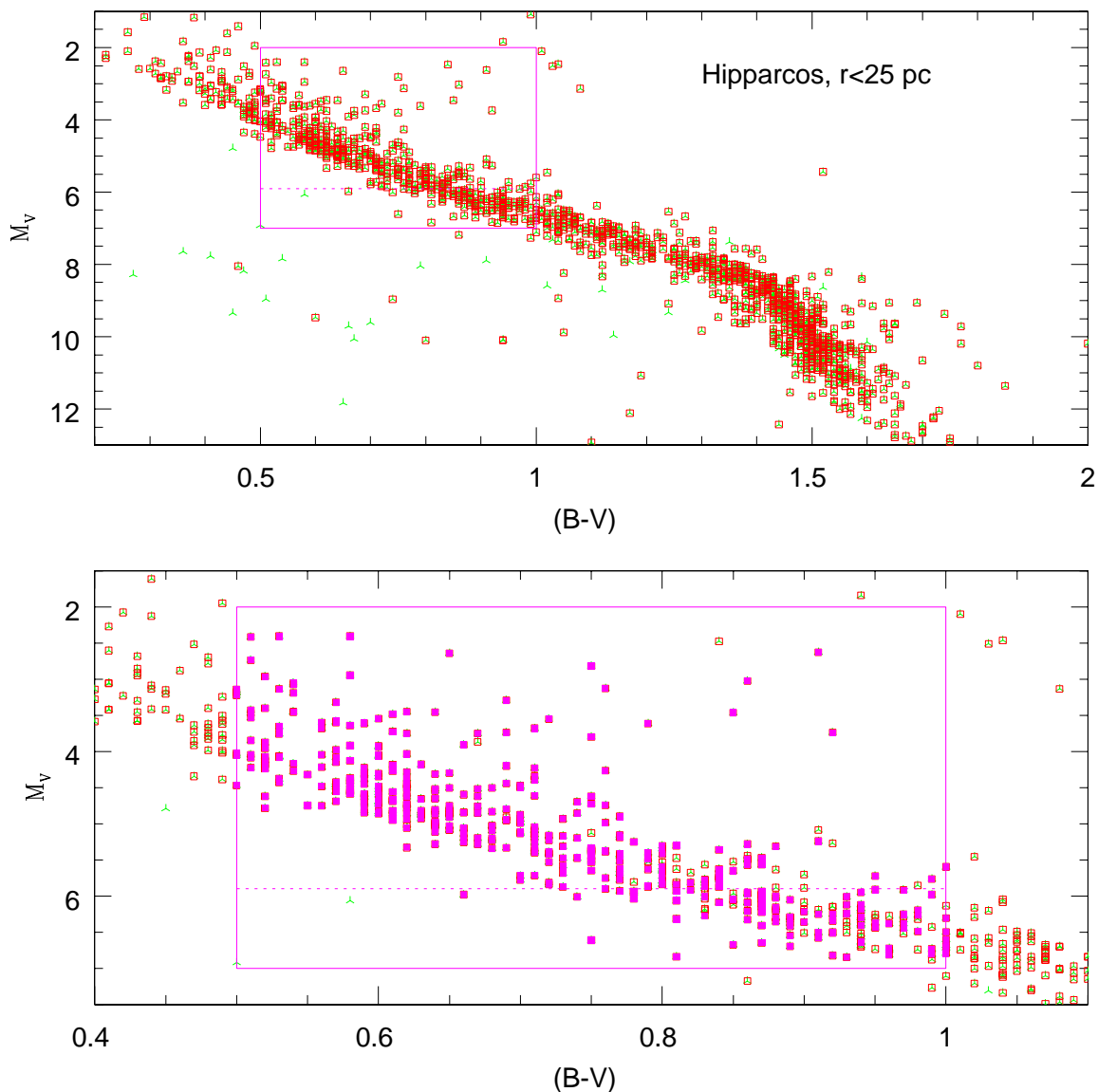


Fig. 4.— The $(M_V, (B-V))$ colour-magnitude diagram defined by 1549 stars in the Hipparcos catalogue with $\pi > 40$ milliarcseconds. Open squares mark 1477 stars with $\frac{\sigma_\pi}{\pi} < 0.2$; almost all of the stars lying below the main-sequence have low-accuracy parallax measurements. The box outlines the limits of the FGK25 sample and the dotted line shows the all-sky completeness limit. Solid squares in the lower panel mark stars with Strömgen photometry.

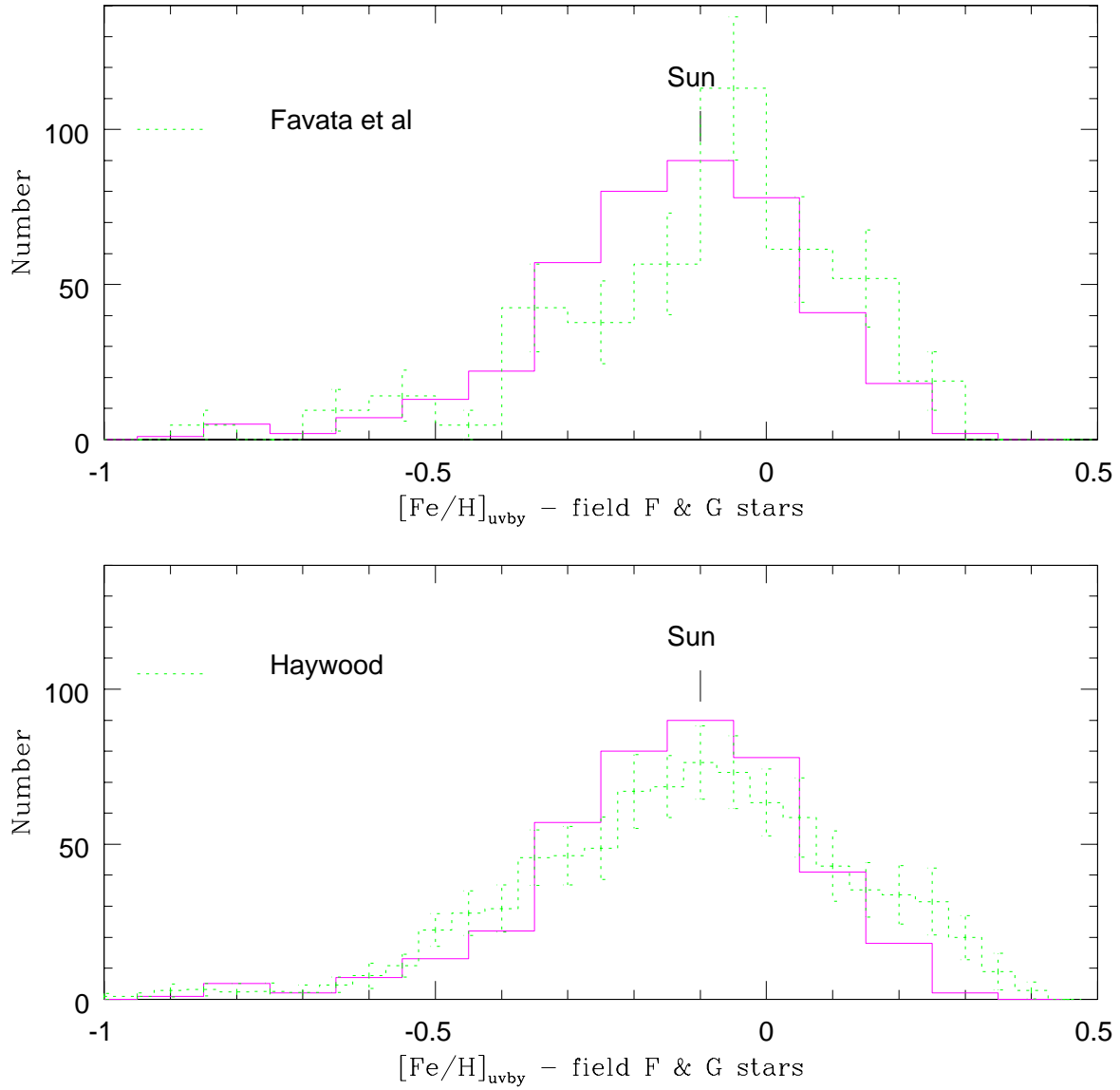


Fig. 5.— Comparison of the abundance distributions derived for the FGK25 dataset and the analyses by Favata *et al.* (1997) and by Haywood (2001). See text for discussion.

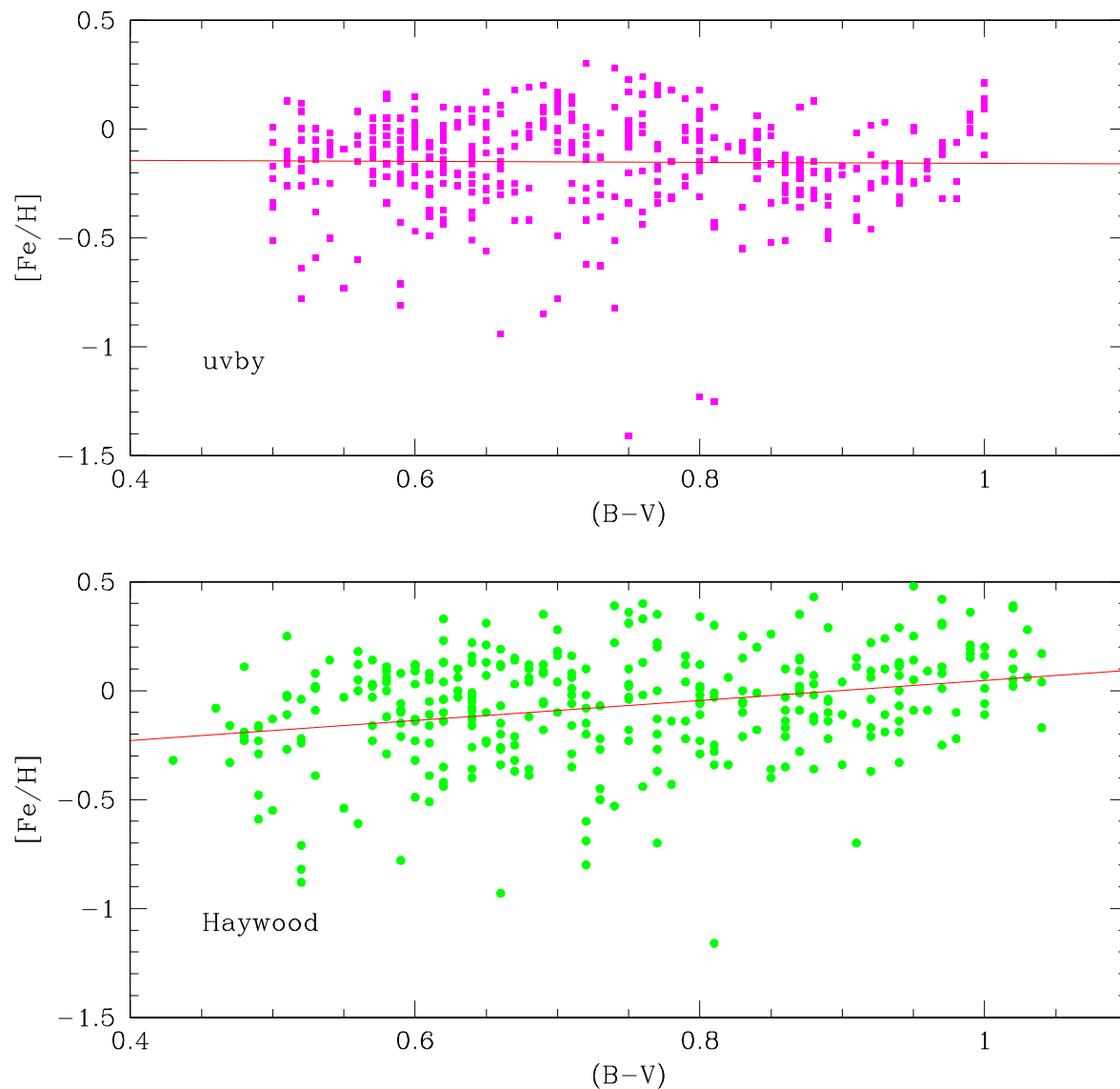


Fig. 6.— The abundance distribution as a function of $(B-V)$ colour for stars in the FGK25 dataset and for the long-lived, $M_V > 4.5$ main-sequence stars in Haywood’s (2001) analysis. The latter stars show a clear trend, with $\langle [Fe/H] \rangle$ increasing with $(B-V)$, suggesting a possible systematic error in the metallicity calibration of Geneva photometry.

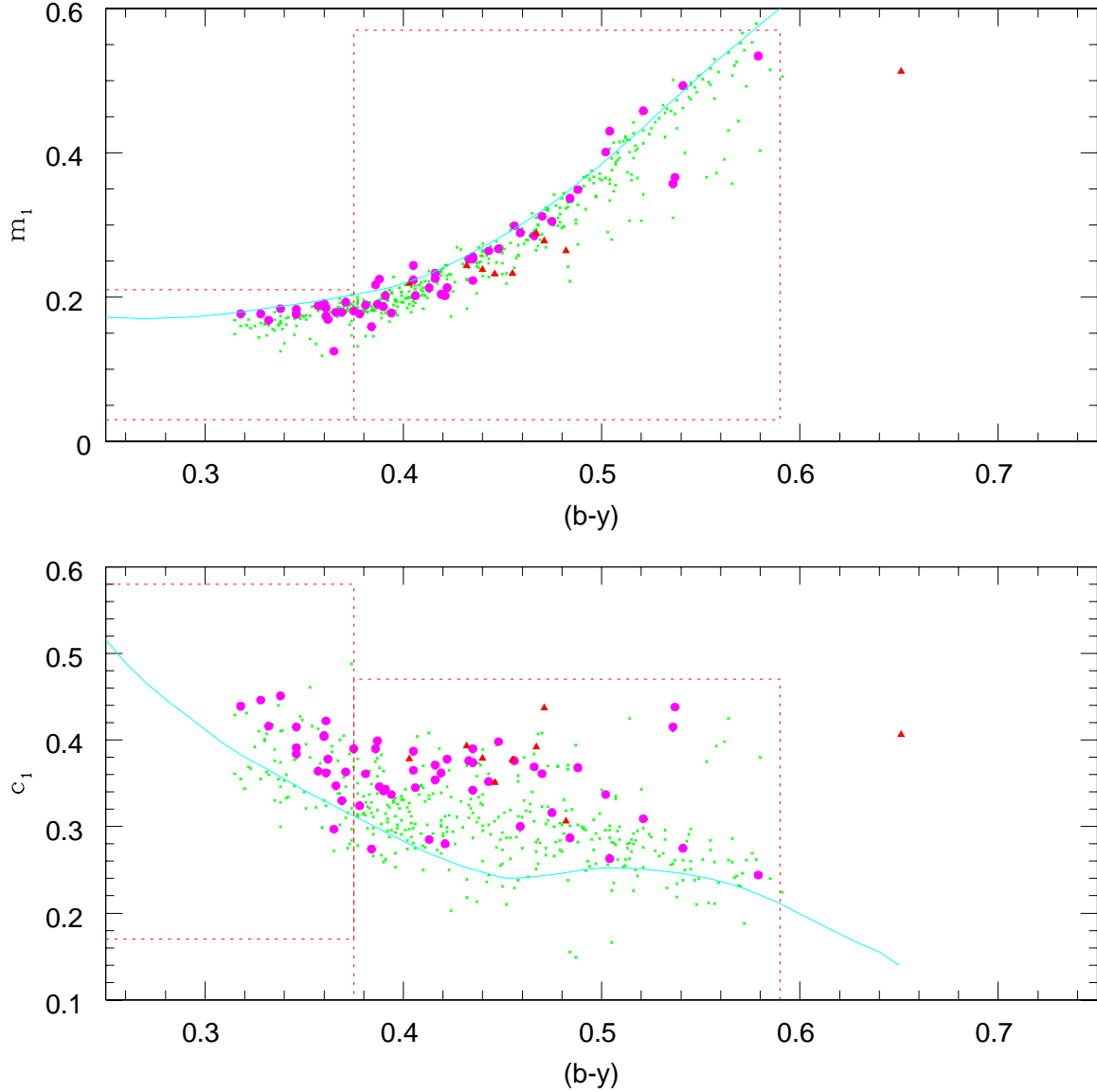


Fig. 7.— Strömrgren data for the FGK25 Hipparcos sample (crosses) and the ESP host stars (solid points). Stars from the latter sample identified as possible subgiants, based on their location in Figure 1, are plotted as solid triangles. The dotted lines mark out the F-star and G-star calibration régimes from Schuster & Nissen (1989). HIP 19221, or HD 27442, is the only ESP host which lies outwith these limits. The solid line plots the fiducial main-sequence, combining data from Davis Philip & Egret (1980) and Olsen (1984).

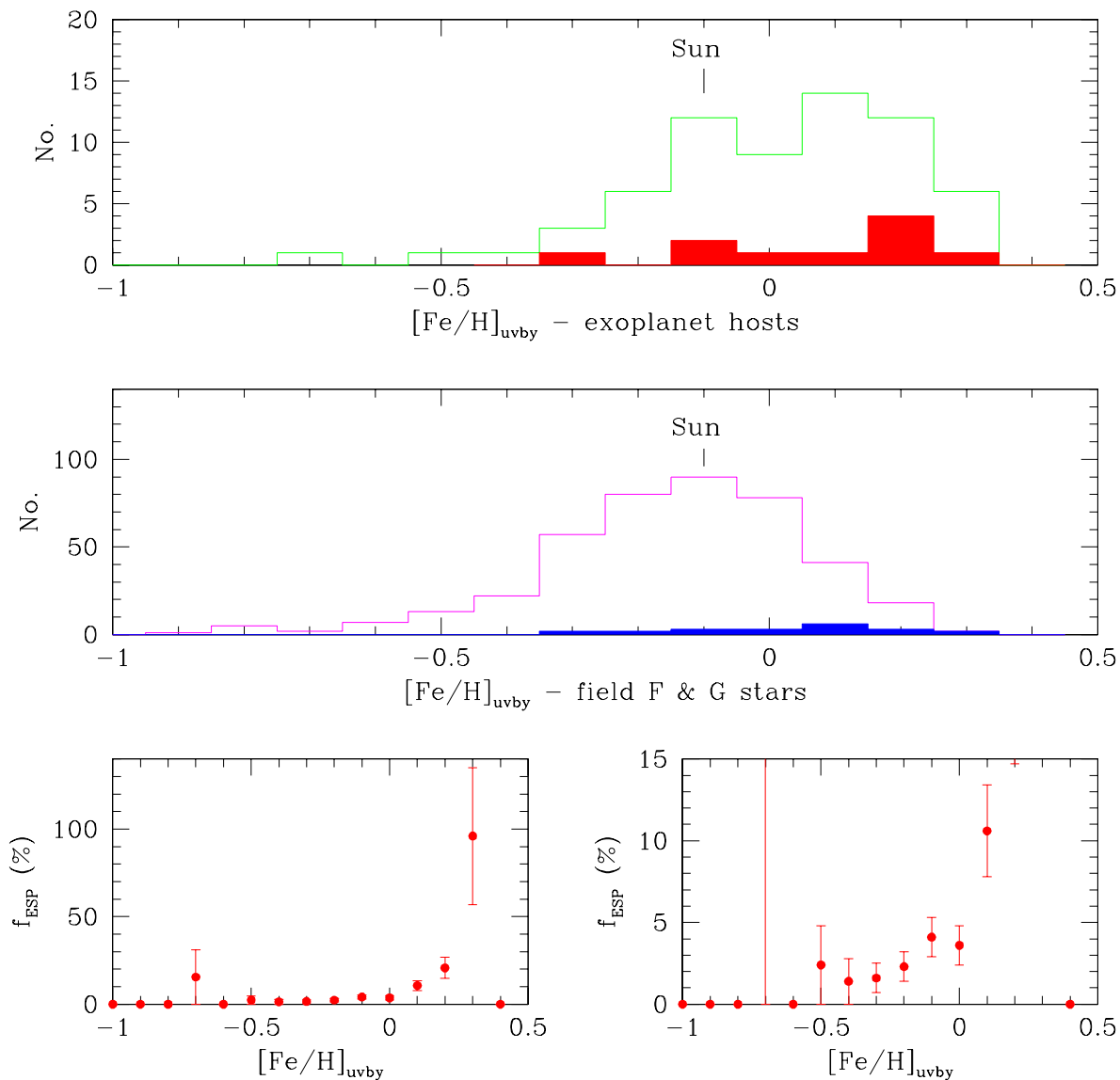


Fig. 8.— The upper panel plots the abundance distribution of the ESP host stars, with solid histogram making the contribution from stars identified as subgiants in Table 1. The middle panel plots the comparable distribution for the FGK25 sample. In both cases, we use the Strömgen abundance calibration, which places the solar abundance at approximately -0.1 dex. The lowest two panels show the fraction of ESP host stars as a function of abundance, scaling the full sample to 5% of the FGK25 sample; the two panels plot identical data, with the vertical scale extended in the right hand panel.

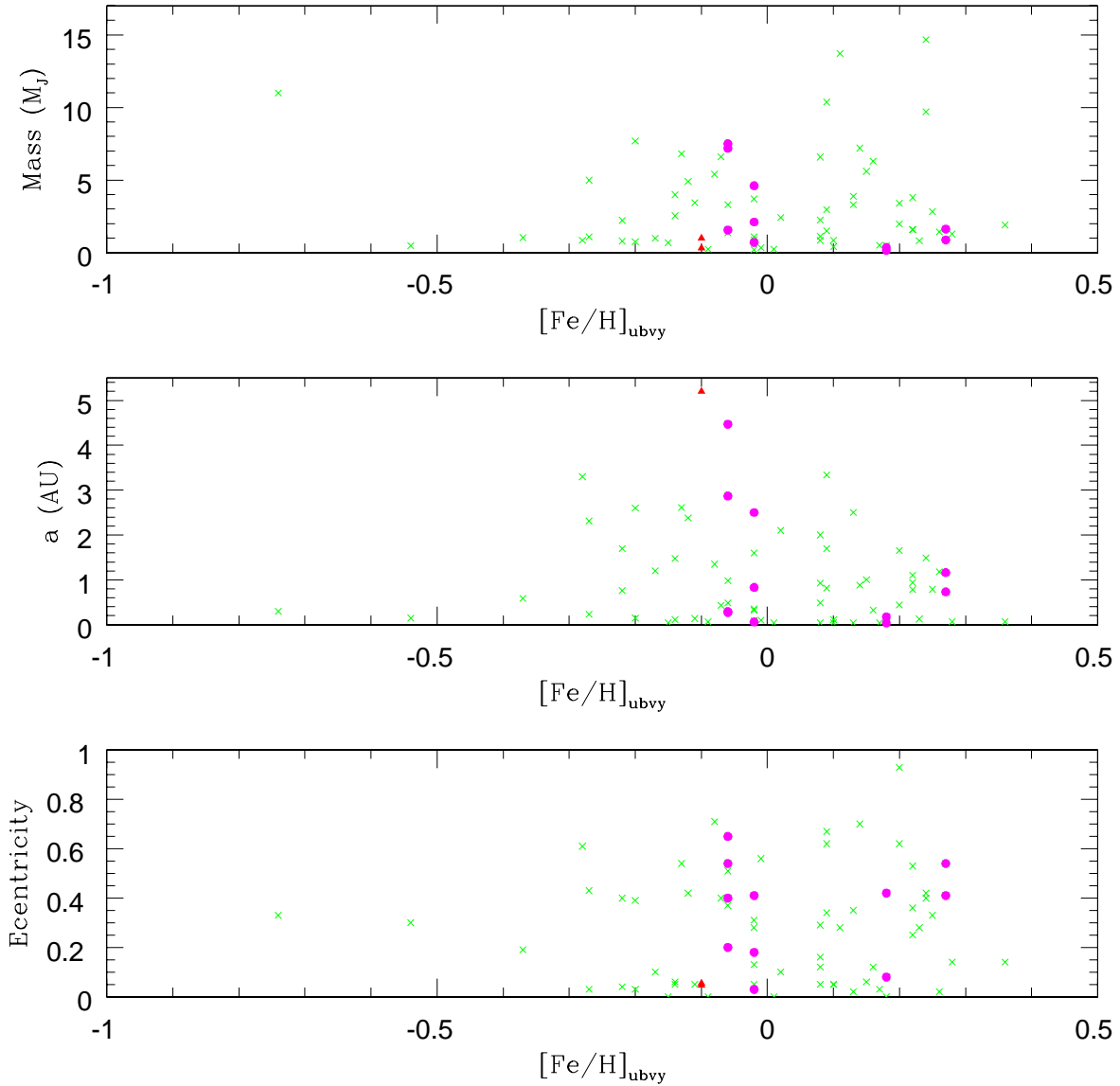


Fig. 9.— The distribution of properties of the known extrasolar planetary systems as a function of abundance. Solid points identify systems with multiple planets; Jupiter and Saturn, representing the solar system, are plotted as solid triangles. HD 114762b, the probable brown dwarf, is the most metal-poor object plotted here.

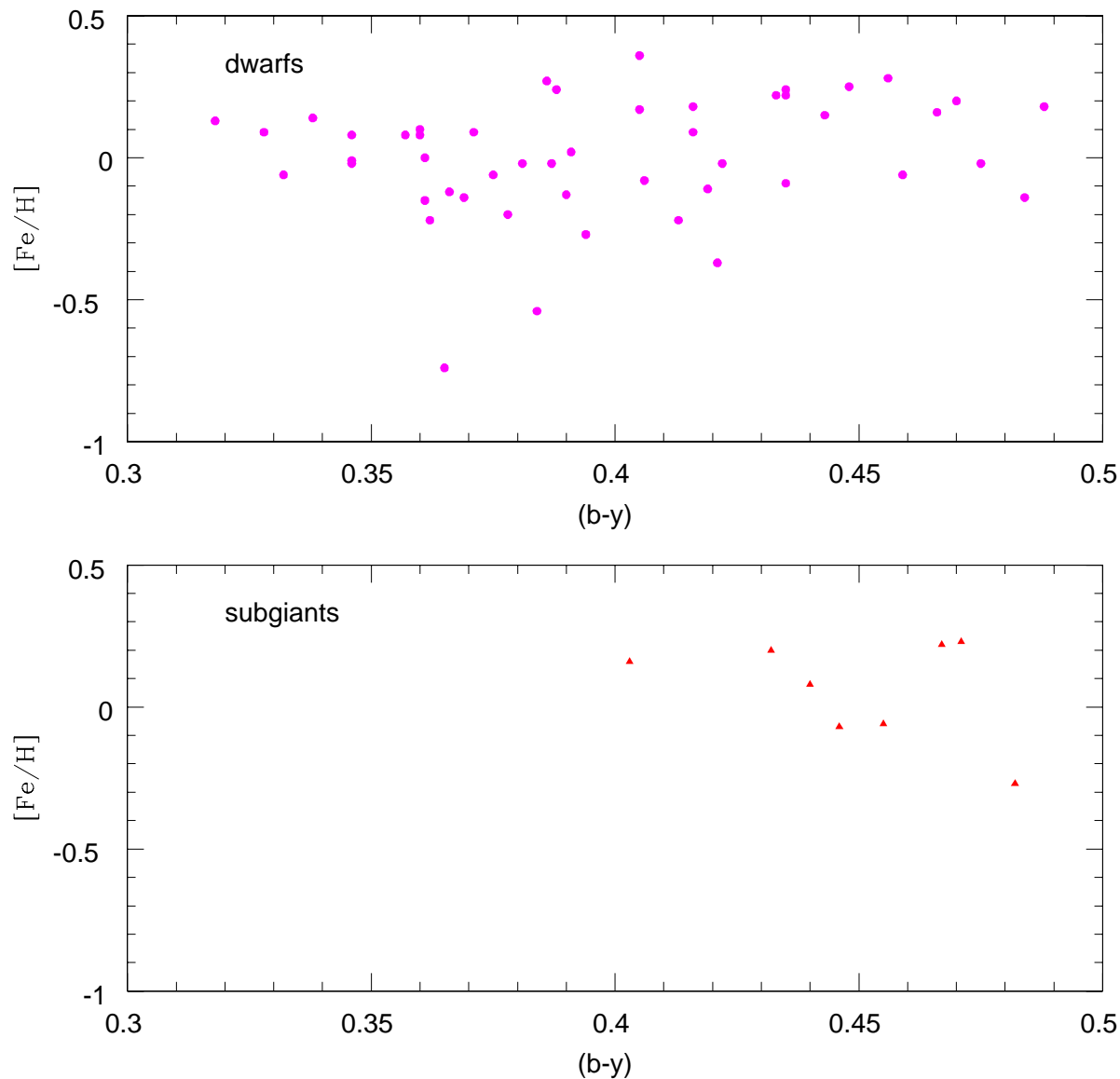


Fig. 10.— The metallicity distribution of the ESP hosts plotted as a function of (b-y) colour, separating stars classed as main-sequence and subgiants based on their location in Figure 1. As Santos *et al.* (2001) point out, there is no evidence for a decrease in the maximum abundance as a function of colour amongst the dwarfs; nor is there evidence for lower abundances amongst the subgiants. Both results argue against the ESP host stars acquiring high metallicities through planetary pollution.

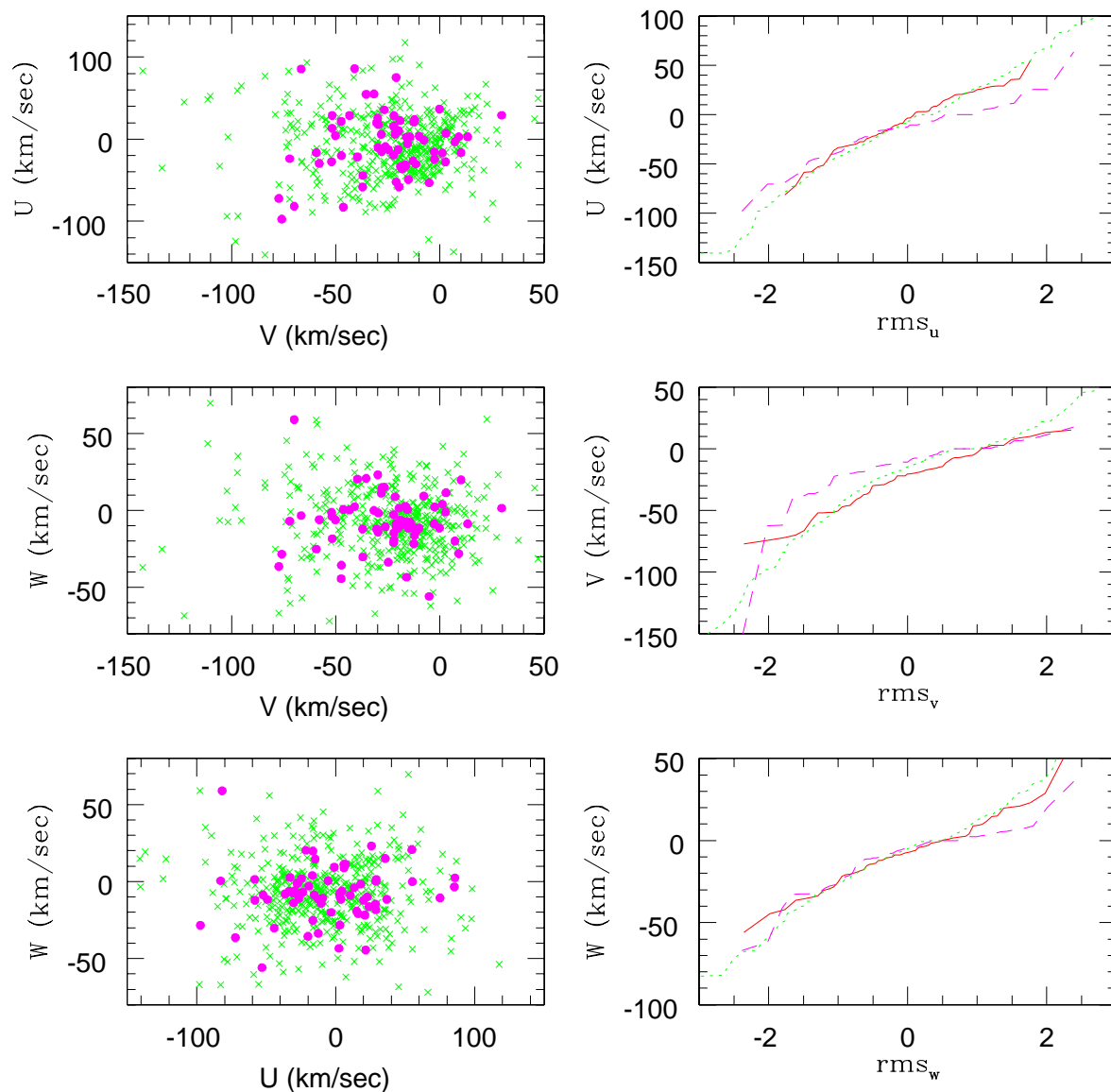


Fig. 11.— Comparison between the space motions of the ESP hosts stars and local disk dwarfs. The left-hand panels plot the two-component velocity distributions for the ESP hosts (solid points) and the volume-complete M-dwarf sample (crosses) from the PMSU. The right-hand panels show probability plots for the ESP hosts (solid line), PMSU M dwarfs (dotted line) and dMe dwarfs (dashed line). A Gaussian distribution gives a straight line, slope σ , in these diagrams.

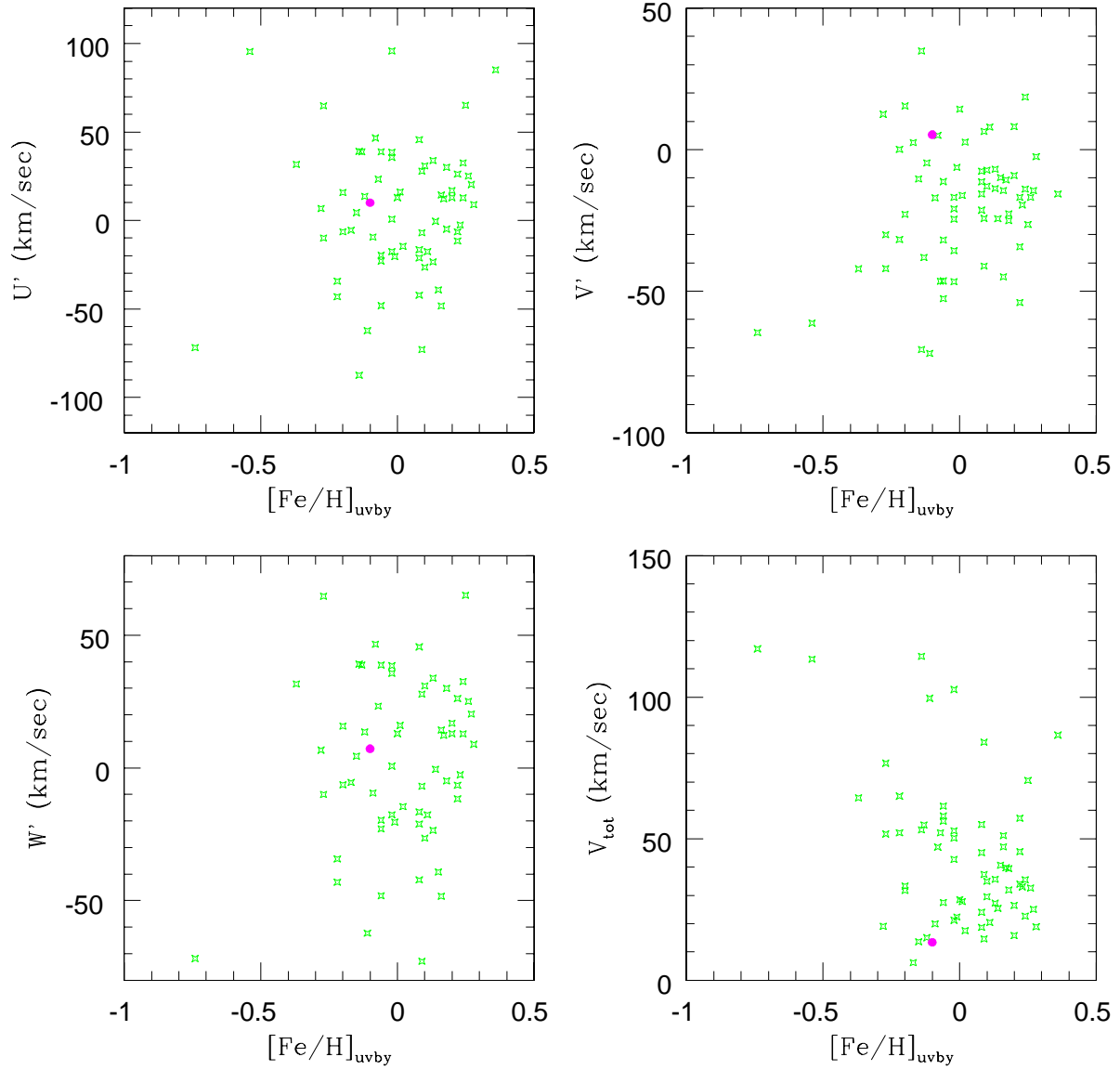


Fig. 12.— The distribution of velocities of ESP host stars with respect to the Local Standard of Rest. The Sun is plotted as a solid point.

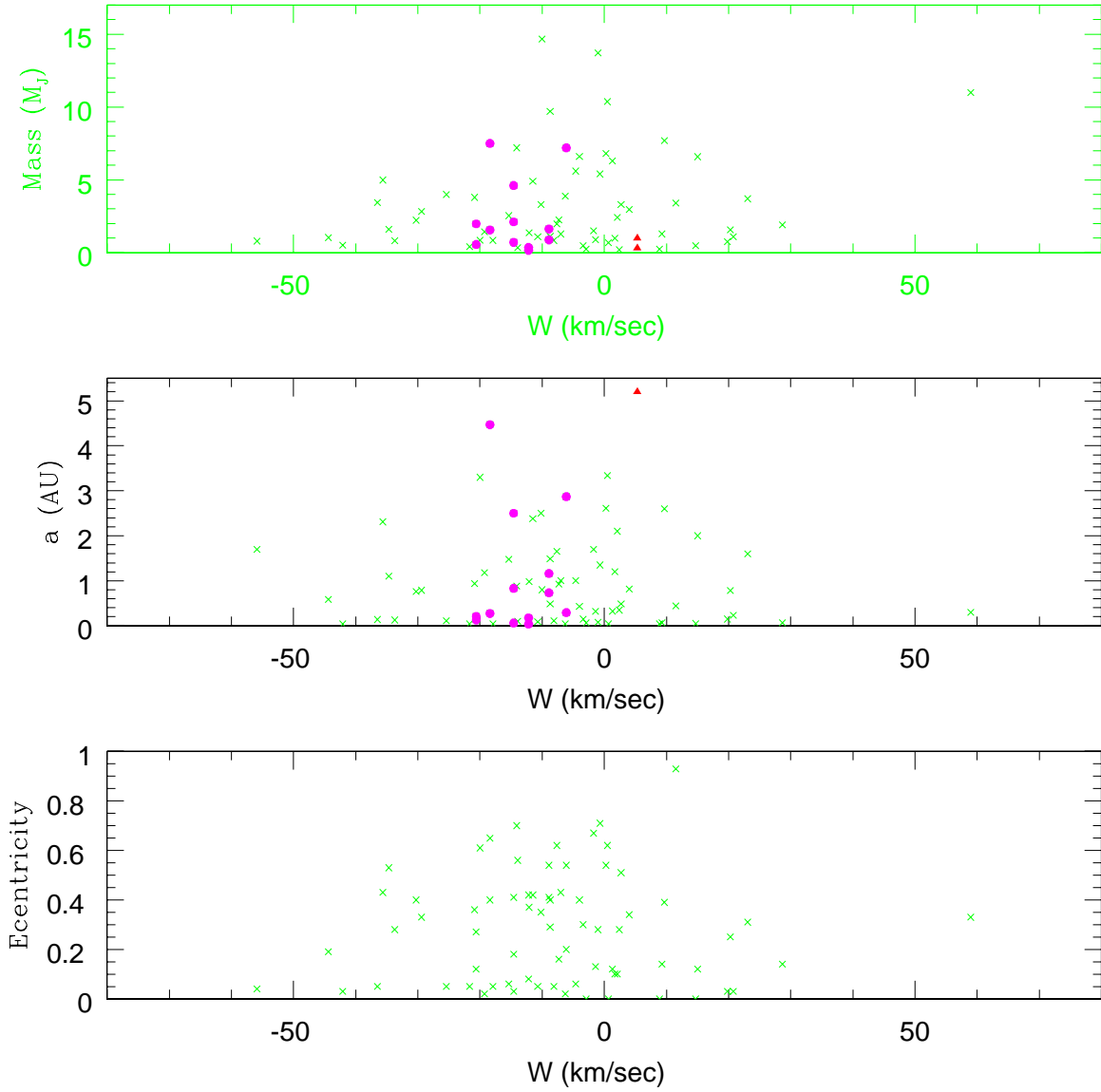


Fig. 13.— The properties of the extrasolar planetary systems plotted as a function of W velocity. The uppermost diagram, plotting planetary mass ($M_2 \sin i$) against W , is the only comparison which shows a suggestion of a trend, with higher-mass systems at low W velocities.